

การออกแบบท่อนำคลื่นสี่เหลี่ยมบรรจุด้วยวัสดุไดอิเล็กตริกที่มีรูอากาศ ด้วยการออกแบบโทโพโลยี  
มุ่งเป้าความถี่ตัดและความกว้างแถบความถี่



บทคัดย่อและแฟ้มข้อมูลฉบับเต็มของวิทยานิพนธ์ตั้งแต่ปีการศึกษา 2554 ที่ให้บริการในคลังปัญญาจุฬาฯ (CUIR)  
เป็นแฟ้มข้อมูลของนิสิตเจ้าของวิทยานิพนธ์ ที่ส่งผ่านทางบัณฑิตวิทยาลัย

The abstract and full text of theses from the academic year 2011 in Chulalongkorn University Intellectual Repository (CUIR)  
are the thesis authors' files submitted through the University Graduate School.

วิทยานิพนธ์นี้เป็นส่วนหนึ่งของการศึกษาตามหลักสูตรปริญญาวิศวกรรมศาสตรมหาบัณฑิต  
สาขาวิชาวิศวกรรมไฟฟ้า ภาควิชาวิศวกรรมไฟฟ้า  
คณะวิศวกรรมศาสตร์ จุฬาลงกรณ์มหาวิทยาลัย  
ปีการศึกษา 2559  
ลิขสิทธิ์ของจุฬาลงกรณ์มหาวิทยาลัย

Designs of rectangular waveguide loaded with air-  
holes dielectric by topology optimization targeting cutoff frequency and bandwidth



A Thesis Submitted in Partial Fulfillment of the Requirements  
for the Degree of Master of Engineering Program in Electrical Engineering

Department of Electrical Engineering

Faculty of Engineering

Chulalongkorn University

Academic Year 2016

Copyright of Chulalongkorn University



สื่อตี เกน : การออกแบบท่อนำคลื่นสี่เหลี่ยมบรรจุด้วยวัสดุไดอิเล็กตริกที่มีรูอากาศ ด้วยการ  
 ออปติไมซ์แบบโทโปโลยีมุ่งเป้าความถี่ตัดและความกว้างแถบความถี่ (Designs of  
 rectangular waveguide loaded with air-holes dielectric by topology  
 optimization targeting cutoff frequency and bandwidth) อ.ที่ปรึกษาวิทยานิพนธ์  
 หลัก: ทับทิม อ่างแก้ว, 71 หน้า.

วิทยานิพนธ์ฉบับนี้นำเสนอการออกแบบเพื่อให้ได้คุณลักษณะการนำคลื่นของท่อนำคลื่น  
 สี่เหลี่ยมที่บรรจุด้วยวัสดุไดอิเล็กตริกพูนที่เหมาะสมที่สุดด้วยระเบียบวิธีทอพอโลยีออปติไมซ์ชัน ได้  
 มีการทดลองแบบวิธีเชิงตัวเลขเพื่อศึกษาโมดและคุณลักษณะดิสเพอชันของท่อนำคลื่นสี่เหลี่ยมที่  
 บรรจุด้วยวัสดุไดอิเล็กตริกพูนโดยใช้วิธีไฟไนต์เอลิเมนต์ จากผลการทดลองแบบวิธีเชิงตัวเลขพบว่า  
 ลักษณะของโมดและคุณลักษณะดิสเพอชันแปรตามความพูนของรูอากาศในเนื้อไดอิเล็กตริกซึ่งได้มี  
 การนิยามให้เป็นค่าตัวประกอบการบรรจุ วิทยานิพนธ์นี้จึงได้มีการนำเสนอแบบจำลองของท่อนำคลื่น  
 สี่เหลี่ยมที่บรรจุด้วยไดอิเล็กตริกพูนด้วยท่อนำคลื่นสี่เหลี่ยมขนาดเดียวกันแต่บรรจุด้วยไดอิเล็กตริก  
 เนื้อเดียวที่มีค่าสภาพยอมประสิทธิผลและได้ทดลองคำนวณในกรณีของท่อนำคลื่นสี่เหลี่ยมที่บรรจุ  
 ด้วยวัสดุไดอิเล็กตริกที่มีรูพูนแบบต่างๆ การใช้แบบจำลองทำให้สามารถออกแบบและหาโครงสร้าง  
 ของไดอิเล็กตริกพูนได้อย่างมีประสิทธิภาพเพื่อให้ได้ค่าคุณลักษณะที่เหมาะสมที่สุดตามจุดประสงค์  
 ของการออกแบบ



ภาควิชา วิศวกรรมไฟฟ้า

สาขาวิชา วิศวกรรมไฟฟ้า

ปีการศึกษา 2559

ลายมือชื่อนิสิต .....

ลายมือชื่อ อ.ที่ปรึกษาหลัก .....

# # 5770530821 : MAJOR ELECTRICAL ENGINEERING

KEYWORDS: POROUS DIELECTRIC-LOADED WAVEGUIDE / COMPOSITE MATERIAL / DISPERSION CHARACTERISTIC / FINITE ELEMENT METHOD / DIELECTRIC-LOADED RECTANGULAR WAVEGUIDE / EFFECTIVE RELATIVE PERMITTIVITY

JEUDY KEAN: Designs of rectangular waveguide loaded with air-holes dielectric by topology optimization targeting cutoff frequency and bandwidth. ADVISOR: ASST. PROF. TUPTIM ANGKAEW, Ph.D., 71 pp.

The design and topology optimization of rectangular waveguides loaded with porous dielectric has been proposed in this thesis. Numerical experiments on modal analysis of rectangular waveguides loaded with various structured porous dielectric made from longitudinal air tubes in lossless dielectric have been carried out by using the finite element method to investigate the modal dispersion characteristics and cutoff frequencies. The results of numerical experiments demonstrate that the dispersion characteristic and cutoff frequencies are depended on the filling factor which is defined as ratio of total area of air tubes to area of waveguide cross section. Thus, an equivalent model of a rectangular waveguide filled with porous dielectric, which is a dielectric-loaded rectangular waveguide of the same cross section with effective permittivity, has been proposed in this work. By using equivalent model, the design and topology optimization targeting cutoff frequency and bandwidth can be achieved effectively.

Department: Electrical Engineering      Student's Signature .....

Field of Study: Electrical Engineering      Advisor's Signature .....

Academic Year: 2016

## ACKNOWLEDGEMENTS

First of all, I would like to take this opportunity to express my deepest gratitude to my advisor, Asst. Prof. Dr. Tuptim Angkaew. She always gives me good advices and comments for conducting this research. Without her, I cannot complete this dissertation. I would also like to thank Dr. Panuwat Janpugdee and Prof. Dr. Apisak Worapishet for being the chairman and external committee for my thesis. I would like to thank to all professors and lecturers at Chulalongkorn University (CU), who have provided me lectures and advices during my study here.

I also thank to all my friends, seniors and juniors in communication laboratory who are always help me during my study here. They share me many research experiences, comments and suggestions to help me solve issues in research.

I, particularly, express my acknowledgement to AUN/Seed-net, JICA project for financial support during my stay here.

Without Institute of Technology of Cambodia (ITC), I cannot be here now. I express my grateful to ITC for giving me a good opportunity to study here, Thailand.

Finally, I would like to express my profound grateful to my parents and family. They have sacrificed and always motivate me all the time of my childhood and study life.

## CONTENTS

	Page
THAI ABSTRACT .....	iv
ENGLISH ABSTRACT .....	v
ACKNOWLEDGEMENTS .....	vi
CONTENTS .....	vii
LIST OF FIGURES .....	1
LIST OF TABLES .....	4
CHAPTER I INTRODUCTION.....	6
1.1. Motivation.....	6
1.2. Objectives.....	7
1.3. Scope of Project.....	8
1.4. Methodology.....	8
1.5. Expected Contribution.....	8
1.6. Organization of dissertation.....	9
CHAPTER II LITERATURE REVIEW .....	10
2.1. Dielectric-loaded rectangular waveguide.....	11
2.2. Modal analysis by Finite Element Method.....	12
2.3. Porosity in material.....	14
2.4. Topology optimization.....	14
2.5. Relative permittivity of Material .....	15
CHAPTER III RESEARCH METHODOLOGY .....	17
3.1. Objective function and model use .....	17
3.2. Ideas from preliminary investigation.....	18

	Page
3.3. Dispersion Graph .....	19
3.4. Methodology used in this research.....	23
3.5. Flow chart for summary of research methodology.....	24
CHAPTER IV RESULTS AND DISCUSSIONS ON INVESTIGATION OF POROUS STRUCTURES.....	26
4.1. Modal Investigation of porous dielectric-loaded rectangular waveguide .....	26
4.2. Validating the results with fully porous dielectric-loaded rectangular waveguide .....	37
CHAPTER V CHARACTERIZATION OF EFFECTIVE RELATIVE PERMITTIVITY OF POROUS DIELECTRIC.....	42
5.1. Case of background material with $\epsilon_r = 2.25$ .....	42
5.2. Case of background material with $\epsilon_r = 3.2$ .....	47
CHAPTER VI APPLICATION AND OPTIMIZING TOPOLOGY OF POROUS DIELECTRIC MATERIAL.....	52
6.1. Application with half porous dielectric-loaded rectangular waveguide.....	52
6.2. Designs by changing topology of porous dielectric to get target cutoff frequency and bandwidth.....	63
CHAPTER VII CONCLUSION .....	66
REFERENCES .....	68
VITA.....	71

## LIST OF FIGURES

Figure 1 Dielectric-loaded rectangular waveguide's cross section; (a) Fully loaded (b) Partially loaded .....	6
Figure 2 Rectangular waveguide and its application .....	11
Figure 3 Example of porosity from nature .....	14
Figure 4 Example of design's structure after applying topology optimization ...	15
Figure 5 Dielectric-loaded rectangular waveguide (a) and the proposed longitudinal porous dielectric-loaded rectangular waveguide (b).....	18
Figure 6 Dispersion graph.....	20
Figure 7 Flow chart summarizing research methodology.....	24
Figure 8 : Cross section of (a) fully dielectric-loaded rectangular waveguide and (b) Longitudinal porous dielectric-loaded rectangular waveguide .....	26
Figure 9 : Cross-section of longitudinal porous dielectric-loaded rectangular waveguide with 18 air tubes embedded in dielectric material .....	27
Figure 10: Dispersion characteristic of modes of porous dielectric-loaded rectangular waveguide with 18 air tubes of different air tube radii. ....	28
Figure 11 Dispersion graph of 18, 32 and 50 Circular holes with filling factor $FF=0.28$ .....	29
Figure 12 Dielectric loaded rectangular waveguide with 18 square holes .....	30
Figure 13 Dispersion characteristic of first two modes of porous dielectric-loaded rectangular waveguide with 18 square and circular air-tubes for $FF=0.5$ .....	31
Figure 14 Dispersion characteristic of first two modes of porous dielectric-loaded rectangular waveguide with $FF=0.12$ , $FF=0.28$ and $FF=0.5$ .....	32
Figure 15 Fully dielectric-loaded rectangular waveguide.....	33

Figure 16 Comparison of dispersion characteristic of the first two modes of porous dielectric-loaded waveguide and fully dielectric loaded waveguide. ....	35
Figure 17 Fully dielectric-loaded rectangular waveguide with $\epsilon_r = 1.86$ .....	38
Figure 18 Fully longitudinal porous dielectric-loaded rectangular waveguide with $\epsilon_r = 2.25$ and $FF = 0.28$ .....	38
Figure 19 Effective permittivity versus frequency for $FF = 0.125$ .....	43
Figure 20 Effective permittivity versus frequency for $FF = 0.1413$ .....	43
Figure 21 Effective permittivity versus frequency for $FF = 0.2$ .....	43
Figure 22 Effective permittivity versus frequency for $FF = 0.28$ .....	44
Figure 23 Effective permittivity versus frequency for $FF = 0.4$ .....	44
Figure 24 Effective permittivity versus frequency for $FF = 0.5$ .....	44
Figure 25 Effective permittivity versus frequency for $FF = 0.6$ .....	45
Figure 26 Effective permittivity versus frequency for $FF = 0.7$ .....	45
Figure 27 Effective permittivity versus frequency for $FF = 0.8$ .....	45
Figure 28 Effective permittivity versus frequency for $FF = 0.9$ .....	46
Figure 29 Graph of average effective relative permittivity versus $FF$ and its fit line for background material $\epsilon_r = 2.25$ by the sample of $FF$ from 0.1 to 0.9 .....	47
Figure 30 Effective permittivity versus frequency for background material $\epsilon_r = 3.2$ in the case of $FF = 0.125$ .....	48
Figure 31 Effective permittivity versus frequency for background material $\epsilon_r = 3.2$ in the case of $FF = 0.2$ .....	48
Figure 32 Effective permittivity versus frequency for background material in the case of $FF = 0.28$ .....	49
Figure 33 Effective permittivity versus frequency for background material $\epsilon_r = 3.2$ in the case of $FF = 0.4$ .....	49

Figure 34 Effective permittivity versus frequency for background material $\varepsilon_r = 3.2$ in the case of FF=0.5.....	49
Figure 35 Effective permittivity versus frequency for background material $\varepsilon_r = 3.2$ in the case of FF=0.6.....	50
Figure 36 Graph of average effective relative permittivity versus FF and its fit line for background material $\varepsilon_r = 3.2$ by the sample of FF from 0.1 to 0.6.....	51
Figure 37 Half dielectric-loaded rectangular waveguide with $\varepsilon_r = 1.545543$ .....	52
Figure 38 Half porous dielectric-loaded rectangular waveguide with $\varepsilon_r = 2.25$ and $FF = 0.5$ .....	53
Figure 39 Plot of error of $\beta/k_0$ versus $k_0a$ for 16 circular holes with FF=0.5.....	54
Figure 40 Plot of error of $\beta/k_0$ versus $k_0a$ for 9 square holes with FF=0.5.....	55
Figure 41 Half dielectric-loaded rectangular waveguide with $\varepsilon_r = 1.86297$ .....	55
Figure 42 Half porous dielectric-loaded rectangular waveguide with $\varepsilon_r = 2.25$ and $FF = 0.28$ .....	56
Figure 43 Plot of error of $\beta/k_0$ versus $k_0a$ for 16 circular holes with FF=0.28..	57
Figure 44 Plot of error of $\beta/k_0$ versus $k_0a$ for 9 square holes with FF=0.28.....	58
Figure 45 Half dielectric-loaded rectangular waveguide with $\varepsilon_r = 2.069255$ .....	58
Figure 46 Half porous dielectric-loaded rectangular waveguide with $\varepsilon_r = 2.25$ and $FF = 0.125$ .....	59
Figure 47 Plot of error of $\beta/k_0$ versus $k_0a$ for 16 circular holes with FF=0.125.....	60
Figure 48 Plot of error of $\beta/k_0$ versus $k_0a$ for 9 square holes with FF=0.125....	61
Figure 49 Plot of error of $\beta/k_0$ versus $k_0a$ for 9 circular holes with FF=0.4.....	62
Figure 50 Plot of error of $\beta/k_0$ versus $k_0a$ for 9 square holes with FF=0.8.....	63

## LIST OF TABLES

Table 1 Comparison of some discrete values of first guiding mode between fully dielectric-loaded rectangular waveguide with $\epsilon_r = 1.86$ and fully porous dielectric-loaded rectangular waveguide with $\epsilon_r = 2.25$ and $FF = 0.28$ .....	39
Table 2 Comparison of some discrete values of second guiding mode between fully dielectric-loaded rectangular waveguide with $\epsilon_r = 1.86$ and fully porous dielectric-loaded rectangular waveguide with $\epsilon_r = 2.25$ and $FF = 0.28$ .....	41
Table 3 Average value of effective relative permittivity versus FF for background material $\epsilon_r = 2.25$ .....	46
Table 4 Average effective relative permittivity versus filling factor FF for background material $\epsilon_r = 3.2$ .....	50
Table 5 Comparison of some discrete values of first guiding mode between Half dielectric-loaded rectangular waveguide with $\epsilon_r = 1.545543$ and fully porous dielectric-loaded rectangular waveguide with $\epsilon_r = 2.25$ and $FF = 0.5$ for 16 circular holes .....	53
Table 6 Comparison of some discrete values of first guiding mode between Half dielectric-loaded rectangular waveguide with $\epsilon_r = 1.545543$ and fully porous dielectric-loaded rectangular waveguide with $\epsilon_r = 2.25$ and $FF = 0.5$ for 9 square holes .....	54
Table 7 Comparison of some discrete values of first guiding mode between Half dielectric-loaded rectangular waveguide with $\epsilon_r = 1.86297$ and fully	

porous dielectric-loaded rectangular waveguide with $\varepsilon_r = 2.25$ and $FF = 0.28$ for 16 circular holes.....	56
Table 8 Comparison of some discrete values of first guiding mode between Half dielectric-loaded rectangular waveguide with $\varepsilon_r = 1.86297$ and fully porous dielectric-loaded rectangular waveguide with $\varepsilon_r = 2.25$ and $FF = 0.28$ for 9 square holes.....	57
Table 9 Comparison of some discrete values of first guiding mode between Half dielectric-loaded rectangular waveguide with $\varepsilon_r = 2.069255$ and fully porous dielectric-loaded rectangular waveguide with $\varepsilon_r = 2.25$ and $FF = 0.125$ for 16 circular holes.....	59
Table 10 Comparison of some discrete values of first guiding mode between Half dielectric-loaded rectangular waveguide with $\varepsilon_r = 2.069255$ and fully porous dielectric-loaded rectangular waveguide with $\varepsilon_r = 2.25$ and $FF = 0.125$ for 9 square holes.....	60
Table 11 Comparison of some discrete values of first guiding mode between Half dielectric-loaded rectangular waveguide with $\varepsilon_r = 1.662908$ and fully porous dielectric-loaded rectangular waveguide with $\varepsilon_r = 2.25$ and $FF = 0.4$ for 9 circular holes.....	61
Table 12 Comparison of some discrete values of first guiding mode between Half dielectric-loaded rectangular waveguide with $\varepsilon_r = 1.193812$ and fully porous dielectric-loaded rectangular waveguide with $\varepsilon_r = 2.25$ and $FF = 0.8$ for 9 square holes.....	62

## CHAPTER I INTRODUCTION

### 1.1. Motivation

Rectangular waveguides are important equipment in communication system. They are expensive in manufacturing. They are commonly used in short distance communication such as feeder or receiver of signal to/from antenna or satellite's dish. So, these devices can be used in both wired and wireless communication system. Anyway, the dispersion characteristic of conventional rectangular waveguide depends on the width and height of its cross section. In general, waveguide and its connectors are designed to work cooperatively. Rectangular waveguide need to be compatible with standard connectors. So, the manufacture fabricates rectangular waveguide with standard cross section. If they want to designs their own waveguide with desired cross section, they also need to designs new compatible connector. So, changing standard waveguide's cross section is not practical in waveguide's designs. In general, changing the dispersion characteristic of rectangular waveguide is to insert dielectric material fully or partially in its hollow core. By doing this, they create the dielectric-loaded rectangular waveguide.

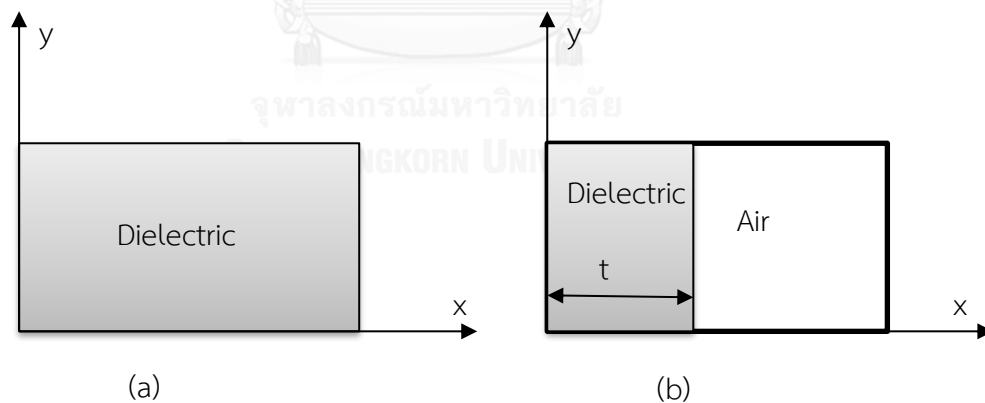


**Figure 1 Dielectric-loaded rectangular waveguide's cross section; (a) Fully loaded (b) Partially loaded**

Dielectric-loaded rectangular waveguide has different dispersion characteristic depending on various type of dielectric material in its core. There are two ways to change the dispersion characteristic of dielectric-loaded rectangular waveguide as well

as cutoff frequency and bandwidth of single mode operation. First method is to change type of dielectric material loaded in waveguide. The second method is to change dimension of dielectric material loaded in waveguide. Figure 1 shows the cross-section of dielectric-loaded rectangular waveguide.

For fully dielectric-loaded rectangular waveguide, we can change only the type of dielectric material to get the desired dispersion characteristic. For partially dielectric-loaded rectangular waveguide, we can change either the type of dielectric material or the dimension “t” of dielectric material. However, dielectric material with required permittivity is difficult to obtain. This is the first constraint in the designs. Usually, various kinds of dielectric materials have different value of dielectric loss depending on operation frequency. Although we can find the required value of permittivity, we cannot ensure that it is also low loss dielectric material in waveguide’s operation frequency. This is also one of constraints in waveguide designs.

Recently, the porosity of dielectric material catches the attention of some researchers because of its ability to leverage the permittivity of medium. Small pores in this medium affect the guiding mode of electromagnetic wave that propagates through them. Surprisingly, one composite material with porosity structure can be considered as one dielectric material with specific relative permittivity called effective permittivity. This medium property can provide us the way to change the dispersion characteristic of dielectric-loaded waveguide. This will benefit us in waveguide designs. In this thesis, we will perform the study on porous structure. We will study the effect of pores’ parameters on the effective permittivity. These parameters will be used in the dielectric-loaded rectangular waveguide’s designs.

## 1.2. Objectives

Our research’s objectives are described as follows:

1. To investigate how the dispersion characteristic of waveguide varies due to the variation of pores’ parameter in the porosity of dielectric material
2. To find the designs’ parameters of porosity that have the major effect on the cutoff frequency and bandwidth of guiding wave

3. To find the relation between the effective permittivity of composite material and pore's parameters
4. To designs the proposed waveguide with target cutoff frequency and bandwidth by optimizing the topology of the porous structure dielectric material loaded in the waveguide

### **1.3. Scope of Project**

The scope of this thesis is limited to the following issues:

1. Study on the porosity structure of dielectric material that is the combination of air-holes and dielectric.
2. The cross-section of waveguide assumes to be rectangular and fully or partially loaded with dielectric material.
3. We focus on how to change topology of waveguide for targeting cutoff frequency and single-mode bandwidth of the proposed waveguide.

### **1.4. Methodology**

1. Reviewing the dispersion characteristic of rectangular waveguide and dielectric-loaded rectangular waveguide
2. Using Numerical method for modal analysis of waveguide with porous dielectric material in waveguide's cross-section
3. Proposing the structure of fully and partially longitudinal porous dielectric-loaded rectangular waveguide
4. Using optimization technique by changing topology of dielectric material for targeting cutoff frequency and bandwidth of the proposed waveguide.

### **1.5. Expected Contribution**

After finishing this project, we will find the way for arranging the porous structure in the dielectric material to obtain desired cutoff frequency and bandwidth of the dielectric-loaded rectangular waveguide. These results are not only contributed to the designing of dielectric-loaded rectangular waveguide but are also practical in different electromagnetic devices. Our finding will help in calculation of required holes'

parameters in dielectric material before going to design's procedure. We can save design's time by using the value of parameters from simulation.

### **1.6. Organization of dissertation**

Other parts of this dissertation from chapter 2 to chapter 7 are organized to facilitate in reporting this work clearly. Chapter 2 will review again about the application of dielectric-loaded rectangular waveguide, porous dielectric medium, topology optimization technique, etc. Chapter 3 describes the numerical methods, setting of parameters, and procedure of research work. In Chapter 4, the receiving data from simulation, cutoff frequency of the first and second mode, single-mode bandwidth and value of effective relative permittivity will be presented and the result will be discussed. Chapter 5 will characterize the effective relative permittivity for porous dielectric material. Chapter 6 will show the result of verifying with the application of half porous dielectric-loaded rectangular waveguide with some case of filling factor. Chapter 7 will conclude our work and future work.

## CHAPTER II LITERATURE REVIEW

The miniaturization of waveguide[1] by maintaining the specification of cutoff frequency of the first mode and the bandwidth of the single-mode operation are desirable for many applications. One practical way of miniaturization can be made by inserting dielectric material into the waveguide such as dielectric-loaded rectangular waveguide [2, 3].

Structure of any waveguide define characteristic of the propagating wave in it. Waveguide's characteristic is strongly depending on the size, width, shape and material properties used in designs. The variation of these parameters can affect the performance of device or change the characteristic of device. They can get the specific propagating characteristic by changing the above parameters to specific value. These parameters' value can be found by calculating with some methods or simulated with some tools or numerical methods.

To use the rectangular waveguide in some application, many researchers try to develop this kind of waveguide by adding the dielectric material (with  $\epsilon_r > 1$ ) in the waveguide's core instead of the air (with  $\epsilon_r = 1$ ) in its hollow core. By doing this, they can create dielectric-loaded waveguide [2, 3] that has different dispersion characteristic depending on inserted dielectric material. Although the sizes of these two kinds of waveguides are the same but they have different characteristic depending on the inserted dielectric material.

Porous structure of dielectric medium in any microwave device is one of the interesting research topics. Advantages of porous structure has been observed and presented in many research works [4-7]. The porous medium is used to change the characteristic of microwave devices. The structure of porous medium is the combination of many small holes in one region. These holes are filled by air or dielectric material to form new structure with high contrast permittivity[4]. Many kinds of porous structures are created by the human or consisted in nature [6]. These special structures affect the electromagnetic wave propagating through them. Hence, it is necessary for analyzing the guiding mode of electromagnetic wave in porous structure of any material in microwave devices [8, 9].

## 2.1. Dielectric-loaded rectangular waveguide

In microwave and millimeter wave application, many kinds of devices are combined for working cooperatively in the communication system. Amongst these devices, waveguides are commonly used as high power transmitters, used in radar equipment and in low noise block converters which located in satellite dishes. There are many different shapes of metallic wall waveguides. Their structure can be rectangular, circular, elliptical cross section, etc. Rectangular waveguides are usually served in application for short connection such as receiver or feeder electromagnetic wave from or to antennas or radars.

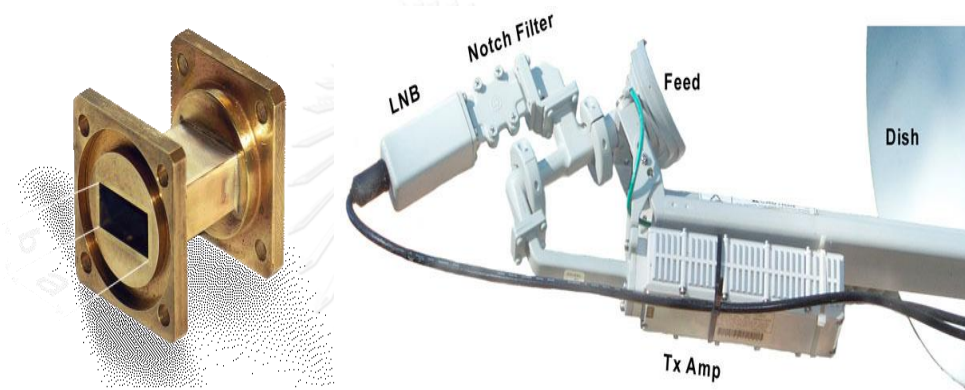


**Figure 2 Rectangular waveguide and its application**

The advantage of waveguide is the ability to carry electromagnetic signal with high frequency (usually higher than 1 GHz). Anyway, waveguide can confine electromagnetic fields to space between its metallic walls (commonly made of copper or brass). This characteristic is useful for supporting the propagation wave without loss or lower loss. The PEC wall of metallic waveguide also protects the inner signal from interferes with outside signal.

Dielectric-loaded rectangular waveguide has been constructed by inserting the dielectric material fully or partially in the hollow core of standard rectangular waveguide. Because of the fixed dimension of standard rectangular waveguide, the characteristic of electromagnetic wave propagating in its hollow core cannot be modified to desirable value. In this sense, dielectric-loaded rectangular waveguide is created for changing the characteristic of guiding wave inside standard waveguide. One advantage of this invention is the ability to change waveguide property without

changing its physical structure. Another advantage is compatibility with standard waveguide connectors. In general, if we want to change the physical structure of the conventional rectangular waveguide, we need to think about how to design its compatible low-loss connector as well. This procedure is not applicable in designs because the manufacture process will become very expensive for changing several devices at the same time.

Anyway, dielectric-loaded rectangular waveguides have been used in many applications. Some are used as dielectric resonators and applicable as sensors for evaluation of small flaws on the surface of metals [10] and measurement of complex dielectric properties of concrete [11]. It is also used to stabilize the frequency and for permittivity measurement of dielectric materials [12]. The other dielectric-loaded resonator's application is to filter only the desirable electromagnetic wave with a specific frequency band around the resonant frequency [13]. Some rectangular waveguides are used to feed the electromagnetic signal to the antenna and satellite's dish [14]. Some are used in the receiver part as low-noise block converters.

## 2.2. Modal analysis by Finite Element Method

The modal analysis by using the finite element method is a powerful tool. There are many finite element formulations for modal analysis of arbitrarily shaped waveguides. Each formulation can provide us a level of accuracy depending on the specific kind of simulated structure. Among many proposed methods, the finite element formulation based on 4 transverse electromagnetic field components is one of the efficient methods that can eliminate spurious mode solutions. In this research work, the finite element formulation in [15] has been employed to analyze the waveguide loaded with porous dielectric material. The finite element method can be briefly reported again as follows.

Let us consider the guided wave problem of time-harmonic electromagnetic field in a uniform waveguide with an arbitrary cross-section. Assume the longitudinal axis of the waveguide be the  $z$ -axis, while the cross-section is in the  $XY$ -plane. The waveguides can be inhomogeneous waveguides filled with arbitrary lossless isotropic materials with scalar permittivity  $\epsilon$  and permeability  $\mu$ . The guided mode solutions in a uniform waveguide along the  $z$ -axis with an arbitrary cross-section can be written as

$$\mathbf{E}(x, y, z) = (\mathbf{e}_t(x, y) + \mathbf{e}_z(x, y))e^{-j\beta z} \quad (2.2.1)$$

$$\mathbf{H}(x, y, z) = (\mathbf{h}_t(x, y) + \mathbf{h}_z(x, y))e^{-j\beta z} \quad (2.2.2)$$

Here, the mode field pattern vector function of electric field is decomposed into transverse component denoted by  $\mathbf{e}_t$  and Z-component denoted by  $\mathbf{e}_z$ . The  $\mathbf{h}_t$  and  $\mathbf{h}_z$  are the transverse component and Z-component of magnetic field mode pattern, respectively.

From the finite element method in [15], the cross-section of waveguide is subdivided into a finite number of elements. The modal functions of transverse electric field component and transverse magnetic field component must make the following variation expression stationary.

$$\beta(\mathbf{e}_t, \mathbf{h}_t) = \frac{A(\mathbf{e}_t, \mathbf{h}_t)}{B(\mathbf{e}_t, \mathbf{h}_t)} \quad (2.2.3)$$

Where

$$A(\mathbf{e}_t, \mathbf{h}_t) = \int_{\Omega} \left\{ \omega \varepsilon \mathbf{e}_t^* \cdot \mathbf{e}_t + \omega \mu \mathbf{h}_t^* \cdot \mathbf{h}_t - \frac{1}{\omega \mu} (\nabla \times \mathbf{e}_t^*) \cdot (\nabla \times \mathbf{e}_t) - \frac{1}{\omega \varepsilon} (\nabla \times \mathbf{h}_t^*) \cdot (\nabla \times \mathbf{h}_t) \right\} ds \quad (2.2.4)$$

$$B(\mathbf{e}_t, \mathbf{h}_t) = \int_{\Omega} \{ \mathbf{i}_z \cdot (\mathbf{e}_t^* \times \mathbf{h}_t + \mathbf{e}_t \times \mathbf{h}_t^*) \} ds \quad (2.2.5)$$

The transverse electric field and magnetic field in each element are expanded as a summation of constant edge based vector shape functions and their corresponding unknown parameters along the edges of triangular elements. By applying the continuity of transverse components of electric field and magnetic field along the edges of elements in the assembling process, and determining the stationary condition of (4), the following eigenvalue system written in matrix form are obtained.

$$[A]\{\Phi\} = \beta [B]\{\Phi\} \quad (2.2.6)$$

By solving (2.2.6), the eigenvalue of propagation constant can be determined. In addition, the mode field pattern can be computed by using corresponding eigenvector of each mode. Hence, the modal solutions and dispersion characteristic of the waveguide can be analyzed.

### 2.3. Porosity in material

Porous dielectric medium is type of medium that one region of specific dielectric material filled by one or many difference materials in many small pores of the background material. Those pores are sorted in random or special form by nature or prepared by human. Some porous mediums are formed by the composition of dielectric material and many small air-holes (those small holes are filled by air). Figure 3 shows one example of porous medium. In this figure, we can see many small air holes that consist in dielectric material.

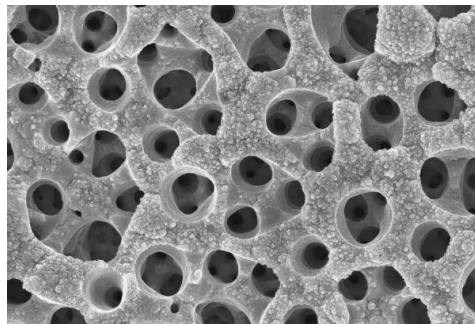


**Figure 3 Example of porosity from nature**

The properties of porous medium are determined by value of dielectric constant of background material, permittivity of dielectric material filled in pores, structure of pores or the shape and size of small pores. These parameters affect the propagation characteristic of electromagnetic wave that propagates through this composite material.

Porous medium can be used as sensor [5, 16] or be waveguide of higher frequency band such as THz-wave [6, 9, 17]. The porosity in dielectric material is also used to strengthen the electric field distribution and to reduce the insulation property of material [18, 19]. These are practical in high-voltage's applications.

### 2.4. Topology optimization

Topology optimization is the special procedure of using mathematic expression and algorithms to minimize or maximize the targeted function to the desirable value by finding or determining the require value of physical structure of material such as shape, density distribution or lattice. Usually, this optimization is used in the aim of

minimizing the design's material or design's cost. Anyway, they also used it for optimizing performance of designed devices. This procedure need to do in the set of limit domain of the designation because we cannot find global optimum easily in the open design's domain. So, designs' parameters will be found between specific domains or by some constraint. These optimization techniques are commonly used in civil and mechanical engineering for structural designs. Figure 4 show one example of material structure after optimizing.



**Figure 4 Example of design's structure after applying topology optimization**

In [20], topology optimization is used in the electrical engineering as well. This technique is applied to find the density distribution of inhomogeneous dielectric material that is inserted in the cross section of waveguide. They have used the hybrid edged/nodal based finite element method for the Eigen-value analysis. For the optimization part, they use Sequential linear Programming to reach the desired value of target functions. They successfully optimize the topology of the cross-section of waveguide with many designs example. But inhomogeneous dielectric material with desirable density distribution of relative permittivity is too difficult to find and cannot be use in practical.

In our research work, we want to optimize the topology of the dielectric material loaded in the waveguide by using the porosity in the material. The advantage of this work is that drilling air-tube on waveguide's cross-section along the longitudinal direction of waveguide is more easily and be practical in designs.

## **2.5. Relative permittivity of Material**

Relative permittivity of material is the frequency-dependent dielectric property of materials[21]. Relative permittivity or dielectric constant is the ratio between the permittivity of the medium to the permittivity of free space.

$$\varepsilon_r = \frac{\varepsilon}{\varepsilon_0} \quad (2.5.1)$$

Where  $\varepsilon_0 = 8.85 \times 10^{-12} \text{ F/m}$  is the permittivity of free space.

The characteristics of a dielectric material are determined by the dielectric constant and it has no units.

The research about the relative permittivity and tangent loss in the print circuit board (PCB) show that the value of relative permittivity seems to be stable at high frequency while the value of tangent loss increase with frequency[22]. The relative permittivity is used to calculate the characteristic impedance of Transmission lines in microstrip devices as well as antenna dimensions and geometries.

Many methods have been used for measuring and characterizing the relative permittivity of material.



## CHAPTER III RESEARCH METHODOLOGY

### 3.1. Objective function and model use

In this research, we want to design longitudinal porous dielectric-loaded rectangular waveguide by using numerical method and topology optimization for desirable cutoff frequency and bandwidth. The Numerical method for modal analysis will be used to analyze guiding modes of electromagnetic wave propagates through the proposed waveguide. The proposed structures of waveguides are longitudinal porous dielectric-loaded rectangular waveguides. These structures are developed from the concept of Dielectric-loaded rectangular waveguides by adding porosity in dielectric material. Many simulation model of these new waveguide's structure will be analyzed and discussed. But in the scope of our project, we choose to consider only the composition between dielectric material and air-tube. Figure 5 shows example of dielectric-loaded rectangular waveguide (a) and the longitudinal porous dielectric-loaded rectangular waveguide (b).

MATLAB program will be used for simulation. The simulation model of proposed waveguide will be constructed by using PDETOOL in MATLAB. This MATLAB's tool can provide us 3 important parameters to be the input parameters of Finite Element Method (FEM). The algorithms of simulation program come from the concept of modal analysis of waveguide by Finite Element Method in reference[15]. The waveguide's cross-section has width  $2a$  and height  $a$ , where  $a$  is the parameter representing the unit length. So, the results from simulation will be applicable when we relate it to actual dimension of standard rectangular waveguide.

Topology optimization will be used to find physical parameter of dielectric material loaded in the waveguide. Our target functions are cutoff frequency and bandwidth. We want to optimize these two functions by defining value of air-tubes' parameters in dielectric material.

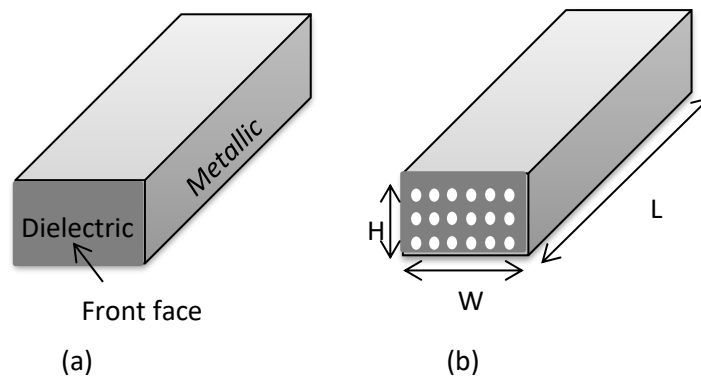


Figure 5 Dielectric-loaded rectangular waveguide (a) and the proposed longitudinal porous dielectric-loaded rectangular waveguide (b)

### 3.2. Ideas from preliminary investigation

From the review of some research works related to the effect of porosity on the dispersion characteristic of electromagnetic wave through porous medium, we have seen the advantages of this structure in microwave, millimeter wave and THz-wave's applications. Generally, the dispersion characteristic of dielectric-loaded rectangular waveguides depend on the value of relative permittivity, dimension and location of dielectric material loaded in the core of rectangular waveguide. While the lower value of relative permittivity is replaced by the higher one, the cutoff frequency will shift to smaller value. The same phenomena also occur while small dimension of dielectric material in the waveguide is replaced with the bigger one. From this concept, they can minimize the size of the conventional rectangular waveguide by inserting dielectric material to its hollow core. They will get smaller dielectric-loaded rectangular waveguide with the same cutoff frequency comparing to the bigger rectangular waveguide.

In preliminary investigation, we try using the porosity in dielectric material filled in half part of rectangular waveguide to change the dispersion graph of half dielectric-loaded rectangular waveguide. Many air-tubes with square shape are drilled in dielectric material along the longitudinal of waveguide. The number and dimension of air-tubes are changed in several simulation models. For fixed-value of  $k_0 a$ , the normalized phase constant  $\beta/k_0$  increase or decrease while the value of material's

permittivity or dimension of dielectric material increase or decrease. In our simulation model for preliminary investigation, we can also increase or decrease the value of normalized phase constant  $\beta/k_0$  with the fixed-value of  $k_0a$  by decrease or increase the number or size of small air-tubes. So, we can get specific value of effective relative permittivity of composite material from specific value of air-tube's parameters. This investigation leads us to research more on the proposed waveguide.

Because drilling small air-tubes with square shape along the longitudinal of waveguide is not practical in designs, we decide to continue our work by finding more results of simulation with circular air-tubes (Circular air-tubes are easier to drill than square air-tubes). Anyway, the fully dielectric-loaded rectangular waveguide will be simulated instead of half dielectric-loaded rectangular waveguide to facilitate the comparison with dispersion relation in the closed-form solution of rectangular waveguide.

### 3.3. Dispersion Graph

In this section, we want to review again the importance of knowing the dispersion graph of waveguide. By plotting the value of normalized phase constant ( $\beta/k_0$ ) versus the multiplication between free space wavenumber and unit length ( $k_0a$ ), we can observe dispersion characteristic of waveguide depending on two important parameters. The first parameter is free space wavenumber ( $k_0$ ). This wavenumber is the parameter of incoming wave to the guiding structure. It relates to the free space wavelength ( $\lambda_0$ ) or the operating frequency ( $f_0$ ). The second parameter is the unit length ( $a$ ). The Unit length represents unit of physical dimension of waveguide. Changing of unit length ( $a$ ) has the same meaning as changing dimension of waveguide. The graph of  $\beta/k_0$  versus  $k_0a$  will tell us how the waveguides operates after the electromagnetic wave with free space wavelength  $\lambda_0$  is inserted into them. In this topic, only the first and second mode of guiding wave is considered and we concentrate only on single-mode bandwidth. The importance thing in this graph is the first and second cutoff value of  $k_0a$  and the shape of the curve of both guiding mode. Figure 6 shows one example of dispersion graph of rectangular waveguide.

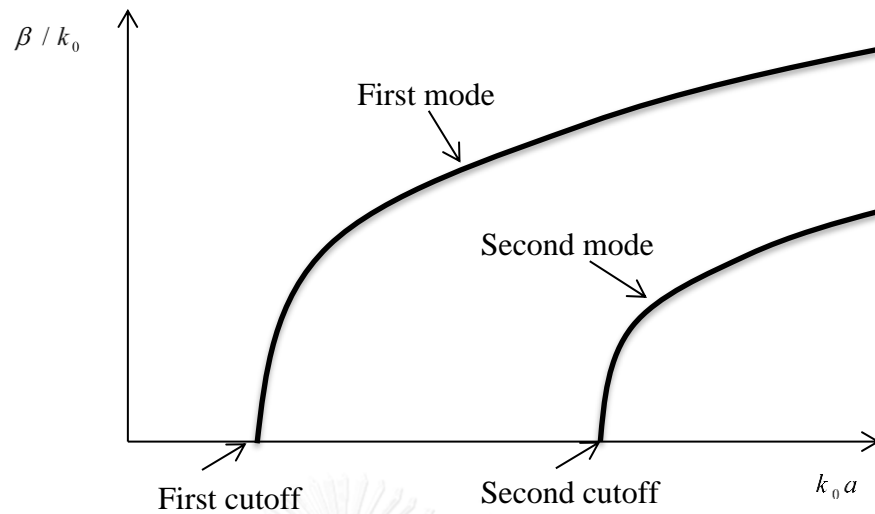


Figure 6 Dispersion graph

This graph tells us that when the value of  $k_0a$  lower than the first cutoff of the first mode, there are no wave that can propagate through this guiding structure. For  $k_0a$  between first cutoff and second cutoff, only one mode with phase constant  $\beta$  that exists and propagates through this structure. For value of  $k_0a$  higher than second cutoff, two or more guiding mode will exist in the waveguide. The wavenumber of the electromagnetic wave related to the wavelength by the formula:

$$k_0 = \frac{2\pi}{\lambda_0} \text{ or } k_0 = \frac{2\pi}{c/f_0} = \frac{2\pi f_0}{c} \quad (3.3.1)$$

Where  $\lambda_0$  and  $f_0$  are free space wavelength and frequency of the incoming wave respectively. The parameter  $c$  is the velocity of light in free space with value  $c \approx 3 \times 10^8 \text{ m/s}$  and related to dielectric properties of free space by formula:

$$c = \frac{1}{\sqrt{\epsilon_0 \mu_0}} \quad (3.3.2)$$

We can say that at any frequency of incoming wave lower than the first cutoff frequency of the device, there is no electromagnetic wave can be guided by waveguide. Between the first and second cutoff frequency, there is only one guiding mode. And for frequency higher than second cutoff frequency, there will be two or more than two guiding modes in waveguide.

The other advantage of choosing the multiplication of the wavenumber  $k_0$  and the unit length  $a$  to be the x-axis in the graph is the possibility of changing any

of these two parameters. In one graph, from the value of  $k_0 a$  at cutoff, if the desirable dimension of waveguide is smaller (or unit length is small), we need the bigger value of  $k_0$ . Inversely, the bigger dimension of waveguide will give us the lower value of  $k_0$ . This means that knowing specific value of cutoff  $k_0 a$  can provide us two options. We can choose either large waveguide with lower cutoff frequency or small waveguide with higher cutoff frequency. If the value of  $k_0 a$  at cutoff decreases, we can get smaller waveguide's dimension with the same cutoff frequency. If the cutoff value  $k_0 a$  increase, we need to design bigger waveguide to get the same cutoff frequency.

Example: Investigation of dispersion graph of most standard hollow core rectangular waveguide with cross-section  $2a \times a$  can give us the ability to find the cutoff frequency of most standard rectangular waveguide with cross-section  $2a \times a$ .

Let plot this dispersion by derive from dispersion relation of rectangular waveguide with cross-section  $2a \times a$ , we will get the graph as similar as Figure 6.

$$\text{From relation } \beta / k_0 = \sqrt{1 - \left( \frac{m\pi}{2k_0 a} \right)^2 - \left( \frac{n\pi}{k_0 a} \right)^2} \quad (3.3.3)$$

$$\text{For } TE_{10}, \text{ at Cutoff } (k_0 a)_{\text{at cutoff}} = \frac{\pi}{2} = 1.5708$$

$$\text{For } TE_{01}, \text{ at Cutoff } (k_0 a)_{\text{at cutoff}} = \pi = 3.1416$$

By knowing value of  $k_0 a$  at cutoff frequency of  $TE_{10}$  and  $TE_{01}$ , we can find cutoff frequency of many standards rectangular waveguide by changing the value of unit length  $a$ .

Example: WR90 has dimension of cross-section as  $2.286\text{cm} \times 1.143\text{cm}$  and WR62 has dimension of cross-section as  $1.58\text{cm} \times 0.79\text{cm}$ . We can find the first and second cutoff frequency of these standard waveguide by just choose unit length  $a$  to  $1.143\text{cm}$  for WR90 and  $0.79\text{cm}$  for WR62. From the relation:

$$(k_0 a)_{\text{first cutoff}} = \left( \frac{2\pi}{\lambda_0} a \right)_{\text{first cutoff}} = \left( \frac{2\pi f_0}{c} a \right)_{\text{first cutoff}} = 1.5708$$

$$(f_0)_{\text{first cutoff}} = \frac{1.5708 \times c}{2\pi a}$$

$$(k_0 a)_{\text{second cutoff}} = \left( \frac{2\pi}{\lambda_0} a \right)_{\text{second cutoff}} = \left( \frac{2\pi f_0}{c} a \right)_{\text{second cutoff}} = 3.1416$$

$$(f_0)_{\text{second cutoff}} = \frac{3.1416 \times c}{2\pi a}$$

For WR90,  $a = 1.143\text{cm}$

Hence,  $f_{0, \text{first cutoff}} = 6.5617\text{GHz}$  and  $f_{0, \text{second cutoff}} = 13.1234\text{GHz}$

For WR62,  $a = 0.79\text{cm}$

Hence,  $f_{0, \text{first cutoff}} = 9.4936\text{GHz}$  and  $f_{0, \text{second cutoff}} = 18.9872\text{GHz}$

Usually, small waveguide operates at high frequency because of its high cutoff frequency or its small cutoff wavelength that is comparable to small dimension of its cross-section. The large waveguide operates in low frequency because of its low cutoff frequency or large cutoff wavelength that is comparable to large dimension of its cross-section.

For same value of cutoff  $k_0 a$ , if we choose small value of unit length  $a$  (it means that we design small waveguide), the value of  $k_0$  at cutoff frequency become large. If electromagnetic wave with low frequency than cutoff frequency is inserted into this small waveguide, the guiding mode cannot exist in this small waveguide. So, small waveguide cannot handle electromagnetic wave with lower frequency than its first cutoff frequency.

Anyway, large waveguide has low cutoff frequency. If the electromagnetic wave propagate at high frequency is inserted into large waveguide, many guided modes can pass through this device. While the value of frequency higher than the cutoff frequency of the large waveguide, many more guiding mode will exist in the waveguide. That is why large waveguide can handle high frequency wave and there will be lots of guiding mode while the value of operate frequency larger than the cutoff frequency of the waveguide.

Various applications in telecommunication system and designs of portable devices, they need the dimension of waveguide as small as possible to save the material and space in the designation of system or circuit board. So, it will be better to get the small value of cutoff  $k_0 a$  in the graph of dispersion.

### 3.4. Methodology used in this research

Before describing the methodology of research, we want to summarize the concept and results from the first investigation. Creating porosity in the dielectric material loaded in rectangular waveguide is the primary concept of our research. From investigation, different structures of the composition between dielectric and air-tubes can provide us specific dispersion characteristic of waveguide with targeted cutoff frequency and bandwidth.

Firstly, we use numerical method for modal analysis to simulate several models of the proposed structure of longitudinal porous dielectric-loaded rectangular waveguide. We will use the results from simulation to find the relationship between cutoff frequency and bandwidth of the proposed waveguide and the physical parameters of air-tube such as location of circle's center, number of circles and radius of circle. After getting the specific relationship, we will use the concept from this relation for optimizing the topology of waveguide.

Secondly, the specific physical parameters of porous medium that can influence the dispersion characteristic of waveguide will be used in optimizing topology of waveguide. The target functions of our optimization are the cutoff frequency and bandwidth of the waveguide. We want to optimize these two functions by changing the topology of air-tubes in the dielectric material loaded in the proposed waveguide. In this step, two groups of dielectric-loaded rectangular waveguide will be studied. The first one is fully dielectric-loaded rectangular waveguide and another one is half dielectric-loaded rectangular waveguide. These two groups of simulation model are chosen because we have the formula of dispersion relation in their closed-form solutions from the analytical method.

### 3.5. Flow chart for summary of research methodology

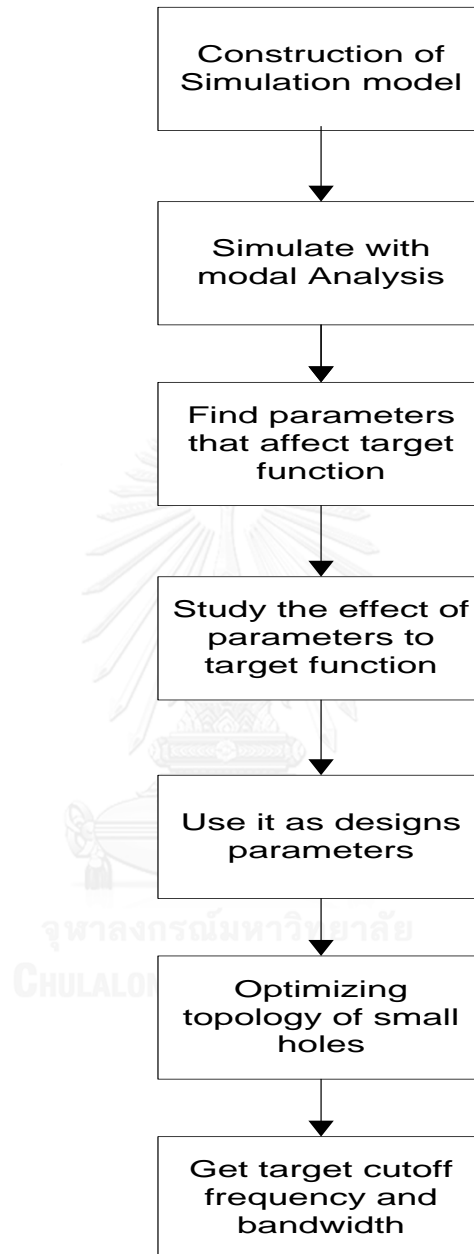


Figure 7 Flow chart summarizing research methodology

Figure 7 shows the flow chart of research methodology. The first step is construction of various simulation model of porous dielectric-loaded rectangular

waveguide with different parameters of circular air-tubes such as number of air-tubes, size of air-tubes and lattice structure of air-tubes. After that we use numerical method for modal analysis to simulate these proposed structures. So, the design parameters and their effects to the propagation characteristic of waveguide will be found. Finally, the design's parameters will be used in order to optimize the target functions which are the cutoff frequency and single-mode bandwidth of the proposed porous dielectric-loaded rectangular waveguides.



## CHAPTER IV RESULTS AND DISCUSSIONS ON INVESTIGATION OF POROUS STRUCTURES

### 4.1. Modal Investigation of porous dielectric-loaded rectangular waveguide

In this section, the Finite Element method is used to simulate the guiding mode of Porous dielectric-loaded Rectangular Waveguide. The results in this section show us the effect of the porosity on the dispersion characteristic of the proposed waveguide. Cross-section's model of fully dielectric-loaded rectangular waveguide is shown in Figure 8 (a). This cross-section is drilled to create air-tubes in the dielectric material along longitudinal of waveguide. By doing this, we can create the longitudinal porous dielectric-loaded rectangular waveguide as shown in Figure 8 (b).

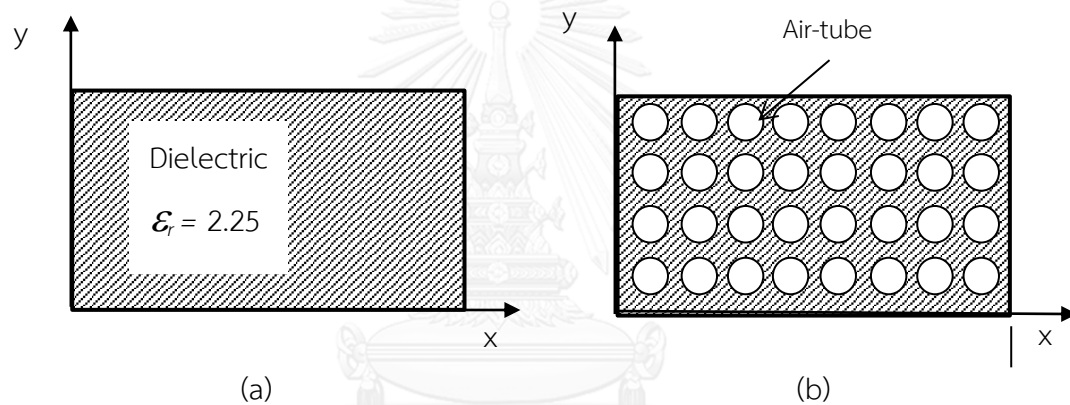


Figure 8 : Cross section of (a) fully dielectric-loaded rectangular waveguide and (b) Longitudinal porous dielectric-loaded rectangular waveguide

The circular air-tubes are created in the dielectric material of fully dielectric-loaded rectangular waveguide with the width to height ratio of 2:1 (cross-section of waveguide is  $2a \times a$ ). If the height  $H$  is choose to be one unit length  $a$  then the width  $W$  is chooes to be two unit of length  $2a$  as shown in Figure 9. The normalized phase constant  $\beta/k_0$  of the guiding mode versus  $k_0a$  is observed.

#### A. The effect of air-tube's radius on waveguide's dispersion characteristic:

Firstly, 18 circular air-tubes are created in the dielectric material on the cross-section along the longitudinal direction of waveguide for numerical experiment. The porous dielectric is comprised of 18 air-tubes embedded in homogenous dielectric of permittivity  $\epsilon_r = 2.25$  as shown in Figure 9. Theses 18 air-tube have been positioned

uniformly on the cross-section of  $2a \times a$ . The radius of air-tube denoted by  $r$  has been selected to investigate its effect on variation of dispersion characteristics. Three cases of modal analysis with different radius  $r$  are:

case 1 :  $r = a/15$  or  $r = 0.06666a$

case 2 :  $r = a/10$  or  $r = 0.1a$

case 3 :  $r = a/7.5$  or  $r = 0.13333a$

where  $a$  is the value of “one unit length”

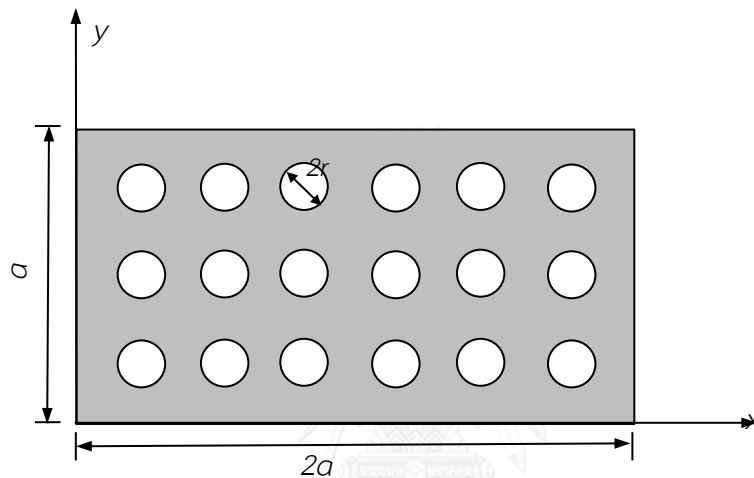


**Figure 9 : Cross-section of longitudinal porous dielectric-loaded rectangular waveguide with 18 air tubes embedded in dielectric material**

The modal analysis of each case is done to find the first 2 guiding mode in the waveguide. The simulation results from all of three cases are plotted together on the same graph. The finite element analysis of modes can be shown in the dispersion graphs as shown in Figure 10. Here,  $\beta/k_0$  denotes the normalized propagation constants, where  $k_0 = \omega\sqrt{\mu_0\epsilon_0}$ . The dispersion graph in Figure 10 demonstrates the normalized propagation constant  $\beta/k_0$  of each guiding mode versus value of  $k_0a$ .

The variation of  $k_0a$  can be regarded as a change of either frequency or the size of the rectangular waveguide. It can be observed that the cutoff frequencies of the fundamental mode can be altered with the radius of air tubes. The smaller the radius of air tube, the cutoff frequency is shifted to lower frequency. In the other word, the waveguide size can be miniaturized while maintaining desirable cutoff frequency. According to the results shown in Figure 10, we may conclude that the cutoff

frequency of the fundamental mode can be changed by inserting of longitudinal porous dielectric in the waveguide.

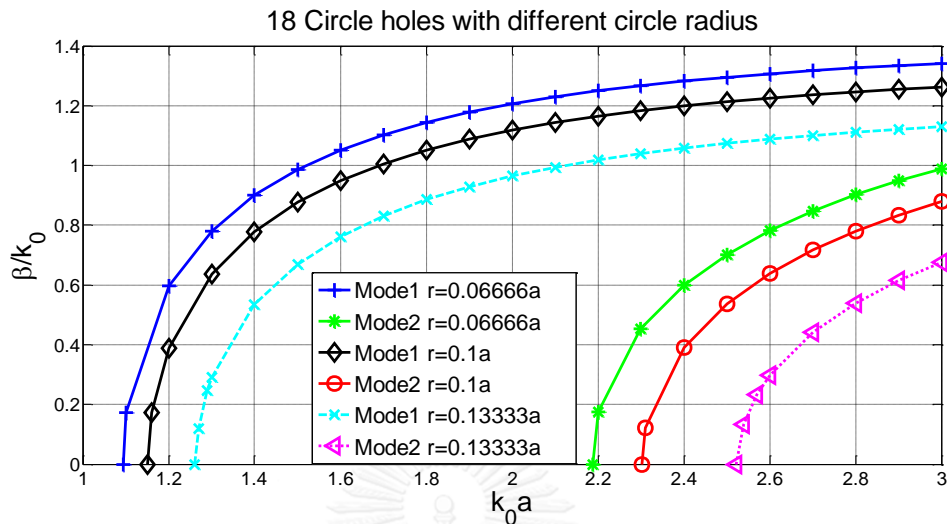


Figure 10: Dispersion characteristic of modes of porous dielectric-loaded rectangular waveguide with 18 air tubes of different air tube radii.

In case 1 ( $r=0.06666a$ ), the graph show that the cutoff frequency of the first and second guiding modes are the lowest compared to case 2 ( $r=0.1a$ ) and case 3 ( $r=0.13333a$ ). The reason is that the cross-section of each circular air-tube in case 1 is smaller than those of each circular air-tube in case 2. The computation of total area of cross-section of all circular air-tubes in each case lead to the conclusion that dispersion graph depends on the total area of cross-section of empty holes (or air-tubes) in dielectric material. The graph shifts to the right side while the radius of the circular air-holes increase or the area of air holes increase.

### B. Effect of number of holes on the dispersion characteristic of waveguides

A parameter indicated the difference of three cases of numerical experiments, demonstrated previously, is called porosity or filling factor which can be defined as follows.

$$FF = \frac{A_{air}}{A} \quad (4.1.1)$$

Here,  $A_{air}$  and  $A$  denote the total area of cross-section of air tubes in the cross-section of waveguide and the area of waveguide cross-section, respectively. The parameter  $FF$  is a measure of the air space in dielectric, and is a fraction of the area of

air-tubes' cross-section over the total cross-section area. The value of  $FF$  is between 0 and 1.

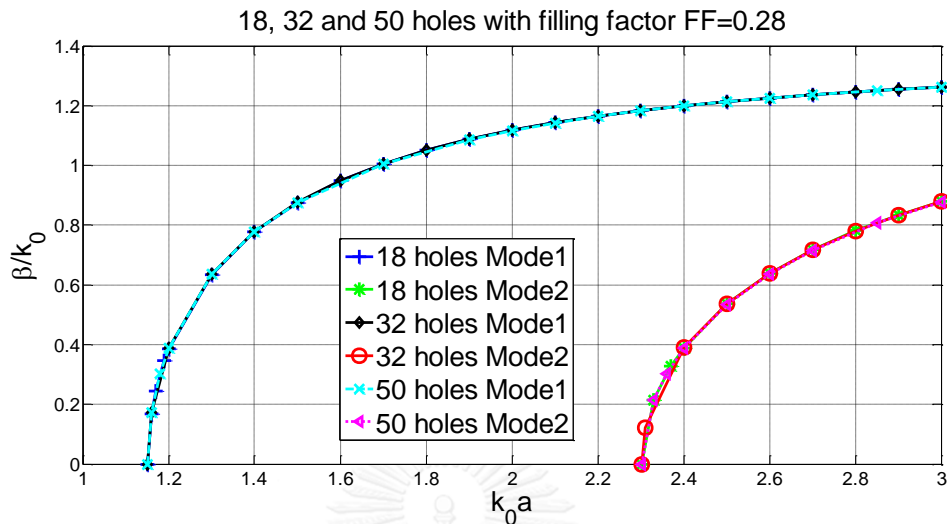


**Figure 11 Dispersion graph of 18, 32 and 50 Circular holes with filling factor  $FF=0.28$**

To investigate further, three cases of numerical experiments on longitudinal porous rectangular waveguides with equally filling factor have been conducted. Three cases of longitudinal porous dielectric with  $FF = 0.28$ , for which the number of air tubes are 18, 32, and 50, have been carried out by the finite element method. The results of dispersion characteristic graphs can be shown in Figure 11. The graphs of dispersion characteristics of three cases with equal Filling factor ( $FF$ ) coincide in spite of the fact that the numbers of air tubes are different. The results can demonstrate that the dispersion characteristic of modes of the porous dielectric-loaded rectangular waveguide depend on the filling factor  $FF$  of porous dielectric. It should be noted that the radius of air tubes is smaller than the guided wavelength.

### **C. Effect of the shape of holes on dispersion characteristic**

The effect of the shape of the air holes is study more in this section. From section B, the assumption is that the graph of guiding characteristic of waveguide depends only on the filling factor ( $FF$ ) of the waveguide.

To probe further on investigation of the effect of  $FF$  to waveguide modal characteristic, another numerical experiment of porous dielectric-loaded rectangular

waveguide with 18 rectangular air tubes, for which  $FF = 0.5$ , has been conducted in comparison with the case of 18 circular air tubes with  $FF = 0.5$ .

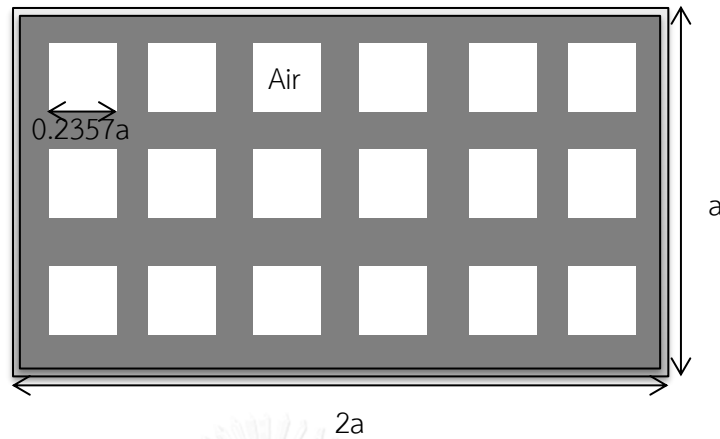


**Figure 12 Dielectric loaded rectangular waveguide with 18 square holes**

Waveguide with 18 square holes is shown in Figure 12. The sides  $h_s$  of each small square in the condition that  $FF=0.5$  is calculated as follow:

- Area of square holes

$$A_s = h_s \times h_s = h_s^2$$

- Area of one square cell

$$A_c = h_c \times h_c = h_c^2$$

$$\text{by } h_c = \frac{a}{3} \Rightarrow A_c = \frac{a^2}{9}$$

- Filling factor is 0.5

$$FF = \frac{A_{s,total}}{A_{c,total}} = \frac{18A_s}{18A_c} = \frac{A_s}{A_c} = \left(\frac{h_s}{h_c}\right)^2 = 0.5$$

$$\Rightarrow h_s = \sqrt{0.5}h_c = \frac{\sqrt{0.5}}{3}a = 0.2357a$$

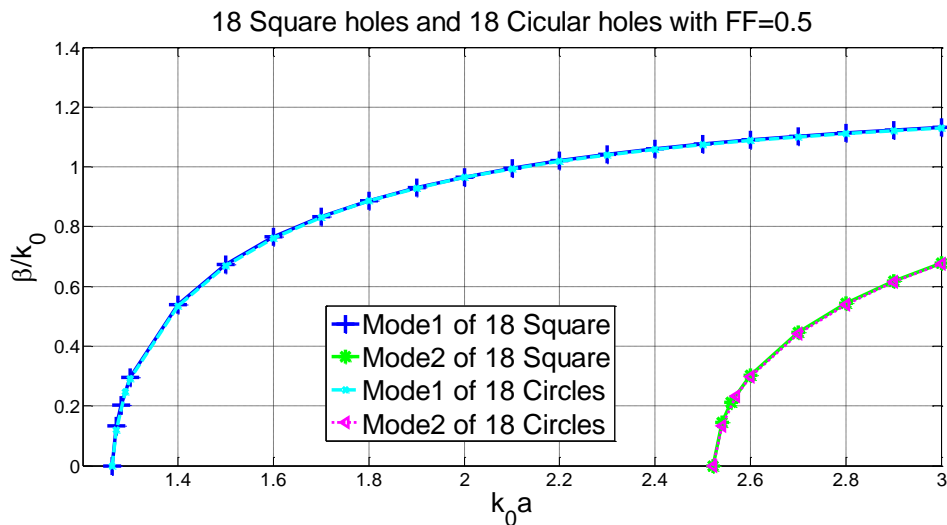


Figure 13 Dispersion characteristic of first two modes of porous dielectric-loaded rectangular waveguide with 18 square and circular air-tubes for FF=0.5

The result of the simulation in this case is shown in Figure 13. The curve of  $\beta/k_0$  versus  $k_0a$  from the simulation of 18 square holes and 18 circular holes are plot together on the same graph. Notice that only the first and second guiding modes are chosen to plot in this graph. The guiding mode 1 and mode 2 of 18 square holes coincide with mode 1 and mode 2 of 18 circular holes respectively. It can be observed that no matter the shape of air tubes are, the modal dispersion characteristic coincide and depend on FF of the porous dielectric.

#### D. Observation on effect of filling factor to dispersion characteristic of waveguide

From the investigation of the dispersion characteristic of porous dielectric-loaded rectangular waveguide carried out in previous experiments, the FF is a key factor to determine the mode characteristic including cutoff frequencies and single mode operation bandwidth. Thus, these results have inspired us to do extra numerical experiments on porous dielectric-loaded waveguides with different FF. We have conducted numerical experiments of porous dielectric-loaded waveguides with FF = 0.12, FF = 0.28, and FF = 0.5, respectively. In these three cases, the size of air-tubes is small compared to the guided wavelength at cutoff frequency of the fundamental mode.

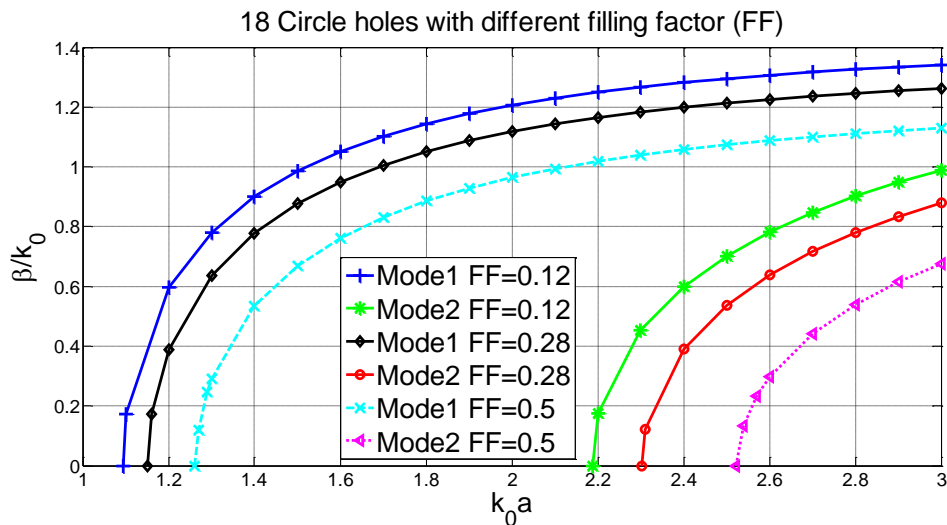


Figure 14 Dispersion characteristic of first two modes of porous dielectric-loaded rectangular waveguide with FF=0.12, FF=0.28 and FF=0.5

The results of dispersion characteristic of the first two modes have shown in Figure 14. We see that the graph shift to the right side or the cutoff frequency increase while the filling factor (FF) of the waveguide increase. The reason is that the present of the air material in the waveguide increase (or the density of air in dielectric material increase) while the value of filling factor become larger. The cutoff frequencies of the first and second guiding mode of the waveguide with large filling factor are also large.

It can be clearly demonstrated that the cutoff frequency of waveguide with higher FF is higher than cutoff frequency of waveguide with smaller FF. According to our knowledge, this is the first time to investigate the effect of porosity to cutoff frequency of the fundamental mode in dielectric-loaded waveguide.

#### E. Relationship of filling factor to the effective relative permittivity of the composite dielectric material

As we have investigated the dispersion characteristic which reveals the nature if porous dielectric-loaded rectangular waveguide, the bandwidth of single mode operation in all cases, which is equal to the difference of cutoff frequency of the first two modes, equals to  $(k_0 a)_c$  at first cutoff, where  $(k_0 a)_c$  denotes the cutoff  $k_0 a$  of the fundamental mode. This modal property is similar to the dispersion characteristic of fully dielectric loaded waveguide where the bandwidth of single mode operation equal

$f_c$  of the first guiding mode. Thus, we compare the mode characteristic of fully dielectric-loaded rectangular waveguide with porous dielectric-loaded rectangular waveguide.

In this section, the cutoff frequency of the first guiding mode in the waveguide from the simulation with Finite Element Method (FEM) and the closed-form solution of the full dielectric loaded rectangular waveguide are used together to find the value of equivalent relative permittivity. This finding value of relative permittivity is used with the closed-form solution to find the value of  $\beta / k_0$  from the assigned value of  $k_0 a$  and to calculate the cutoff value of the second guiding mode. After that the computed result is plot together with the simulated result on the same graph for comparing to each other.

In this point, we review again the dispersion relation of fully dielectric-loaded rectangular waveguide as follow:

The guiding electromagnetic field in the waveguide is written as:

$$\mathbf{E}(x, y, z) = (\vec{e}_t(x, y) + \vec{e}_z(x, y)) e^{-j\beta z} \quad (4.1.2)$$

$$\mathbf{H}(x, y, z) = (\vec{h}_t(x, y) + \vec{h}_z(x, y)) e^{-j\beta z} \quad (4.1.3)$$

With  $\beta$  is the propagation constant ( $rad/m$ ),  $\mathbf{E}(x, y, z)$  and  $\mathbf{H}(x, y, z)$  are the electric field ( $v/m$ ) and magnetic field ( $A/m$ ) respectively. The value of propagation constant  $\beta$  should be real number.

By solving the Maxwell's equations and applying boundary conditions, we obtain mode solution.

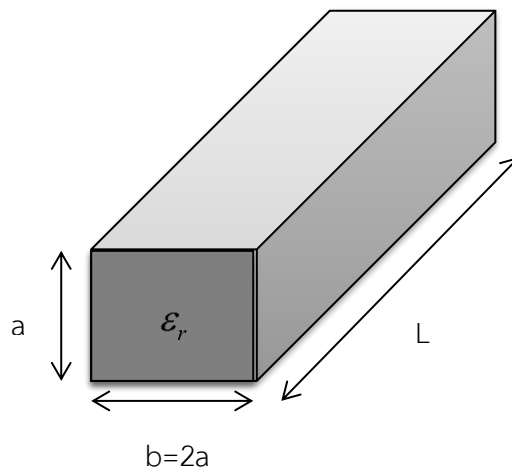


Figure 15 Fully dielectric-loaded rectangular waveguide

Fully dielectric-loaded rectangular waveguide is shown in Figure 15. The closed-form solution of this kind of waveguide is written as follow:

$$\beta = \sqrt{\omega^2 \varepsilon_0 \varepsilon_r \mu_0 \mu_r - \left( \frac{m\pi}{2k_0 a} \right)^2 - \left( \frac{n\pi}{k_0 a} \right)^2} \quad (4.1.4)$$

$$\frac{\beta}{k_0} = \sqrt{\varepsilon_r - \left( \frac{m\pi}{2A} \right)^2 - \left( \frac{n\pi}{A} \right)^2} \quad (4.1.5)$$

Where  $k_0 = \omega^2 \varepsilon_0 \mu_0$  and  $A = k_0 a$

$k_0$  is wavenumber in free space ( $rad/m$ )

$$\varepsilon_0 = 8.854 \times 10^{-12} F/m$$

$$\mu_0 = 4\pi \times 10^{-7} H/m$$

The cutoff of the fundamental mode  $A_{c,TE_{10}}$  occurs when  $m=1, n=0$  and  $\frac{\beta}{k_0} = 0$

$$\begin{aligned} \text{So, } \varepsilon_r - \frac{\pi^2}{4A_{c,TE_{10}}^2} &= 0 \\ \Rightarrow A_{c,TE_{10}} &= \frac{\pi}{2\sqrt{\varepsilon_r}} \end{aligned} \quad (4.1.6)$$

This value  $A_{c,TE_{10}}$  is the first cutoff value of  $k_0 a$  in the dispersion graph of fully dielectric-loaded rectangular waveguide with the relative permittivity  $\varepsilon_r$ .

The second cutoff occurs when  $m=0, n=1$  and  $\frac{\beta}{k_0} = 0$

$$\begin{aligned} \text{So, } \varepsilon_r - \frac{\pi^2}{A_{c,TE_{01}}^2} &= 0 \\ \Rightarrow A_{c,TE_{01}} &= \frac{\pi}{\sqrt{\varepsilon_r}} \end{aligned} \quad (4.1.7)$$

This value  $A_{c,TE_{01}}$  is the second cutoff value of  $k_0 a$  in the dispersion graph of full dielectric-loaded rectangular waveguide with the relative permittivity  $\varepsilon_r$ .

The relative permittivity of dielectric in fully dielectric-loaded waveguide has been calculated by closed-form solution of  $TE_{10}$  modes as:

$$\begin{aligned} \beta/k_0 &= \sqrt{\varepsilon_{eff} - \left( \frac{\pi}{2k_0 a} \right)^2} \\ \Rightarrow \varepsilon_{eff} &= \left( \frac{\beta}{k_0} \right)^2 + \left( \frac{\pi}{2k_0 a} \right)^2 \end{aligned} \quad (4.1.8)$$

After substitute a pair value of  $\beta/k_0$  and  $k_0a$  from first mode of simulation results with  $FF=0.5$ , we found  $\epsilon_{eff} = 1.55$ .

By using dispersion relation again for computing the normalized phase constant of the first and second mode of fully dielectric-loaded rectangular waveguide with  $\epsilon_{eff} = 1.55$ , it is found that the dispersion graphs of fully dielectric loaded waveguide with relative permittivity of 1.55 coincide with the dispersion graphs of porous dielectric-loaded waveguide with  $FF = 0.5$  for the first two modes. The results are shown in Figure 16.

Thus, it can be concluded that porous dielectric-loaded rectangular waveguide with the specific value of filling factor (FF) is equivalent to fully dielectric-loaded rectangular waveguide with specific value of relative permittivity. These results can be applied to design waveguide by adjusting filling factor  $FF$  of porous dielectric.

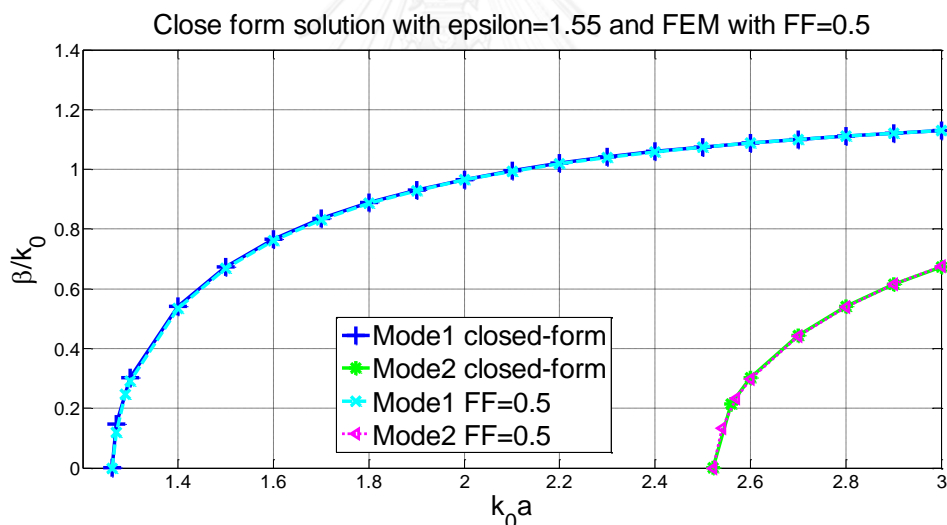


Figure 16 Comparison of dispersion characteristic of the first two modes of porous dielectric-loaded waveguide and fully dielectric loaded waveguide.

#### F. Relationship between hole's radius and wavelength at the first cutoff

We have the relationship between wavenumber and wavelength:

$$k = \frac{2\pi}{\lambda}$$

The radius of each circular hole is:

For case 1  $r = 0.06666a$

For case 2  $r = 0.1a$

For case 3  $r = 0.13333a$

Two cutoff value of  $k_0a$  are known.

In case 1,  $k_0a = 1.1$  at first cutoff and  $k_0a = 2.2$  at second cutoff

In case 2,  $k_0a = 1.155$  at first cutoff and  $k_0a = 2.31$  at second cutoff

In case 3,  $k_0a = 1.27$  at first cutoff and  $k_0a = 2.53$  at second cutoff

Now we focus on each case:

Case 1:

$$r = 0.06666a \Rightarrow a = \frac{1}{0.06666} r$$

$$k_0a = \frac{2\pi}{\lambda} a = \frac{2\pi r}{0.06666\lambda} = 94.2572 \frac{r}{\lambda}$$

At first cutoff

$$k_0a = 1.1 = 94.2572 \frac{r}{\lambda}$$

$$\Rightarrow \frac{r}{\lambda} = 0.01167 \text{ or } r = 0.01167\lambda$$

$$r \approx \frac{1}{85} \lambda$$

At second cutoff

$$k_0a = 2.2 = 2(1.1) = 94.2572 \frac{r}{\lambda}$$

$$\Rightarrow \frac{r}{\lambda} = 2(0.01167) \text{ or } r = 2(0.01167)\lambda$$

$$r \approx \frac{1}{42} \lambda$$

Anyway, the wavelength calculated from the first cutoff is the largest wavelength (the lowest frequency). So, the radius of circular hole must be calculated from the first cutoff. We will get the reasonable value of radius because it is the proportional to the largest wavelength.

From this point, we will calculate the radius only related to the first cutoff value of  $k_0a$ .

Case 2:

$$r = 0.1a \Rightarrow a = \frac{1}{0.1}r = 10r$$

$$k_0a = \frac{2\pi}{\lambda}a = \frac{2\pi 10r}{\lambda} = 62.8318 \frac{r}{\lambda}$$

At the first cutoff

$$k_0a = 1.155 = 62.8318 \frac{r}{\lambda}$$

$$\Rightarrow \frac{r}{\lambda} = \frac{1.155}{62.8318} \text{ or } r = 0.01838\lambda$$

$$r \approx \frac{1}{54} \lambda$$

Case 3:

$$r = 0.13333a \Rightarrow a = \frac{1}{0.13333}r$$

$$k_0a = \frac{2\pi}{\lambda}a = \frac{2\pi r}{0.13333\lambda} = 47.125 \frac{r}{\lambda}$$

At the first cutoff

$$k_0a = 1.27 = 47.125 \frac{r}{\lambda}$$

$$\Rightarrow \frac{r}{\lambda} = \frac{1.27}{47.125} \text{ or } r = 0.02694\lambda$$

$$r \approx \frac{1}{37} \lambda$$

In these three cases, we see that the largest ratio of circle's radius is  $r \approx \frac{1}{37} \lambda$  where  $\lambda$  the largest wavelength of propagation wave in waveguide. We can conclude that the value of circle's radius is so small compare to the wavelength of first cutoff of guiding mode.

#### 4.2. Validating the results with fully porous dielectric-loaded rectangular waveguide

In this point, we will show the results of one more simulations case to find the relationship between filling factor (FF) and effective relative permittivity of composite material.

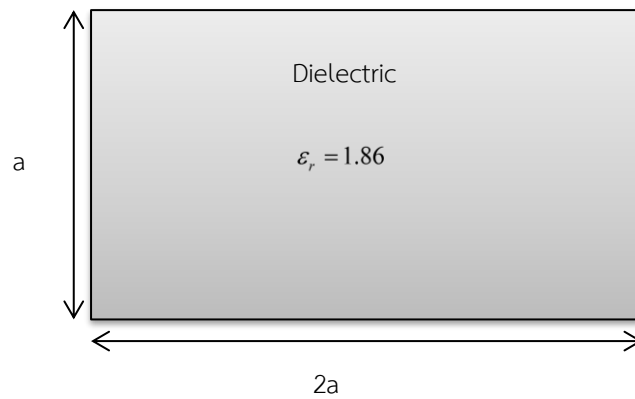


Figure 17 Fully dielectric-loaded rectangular waveguide with  $\epsilon_r = 1.86$

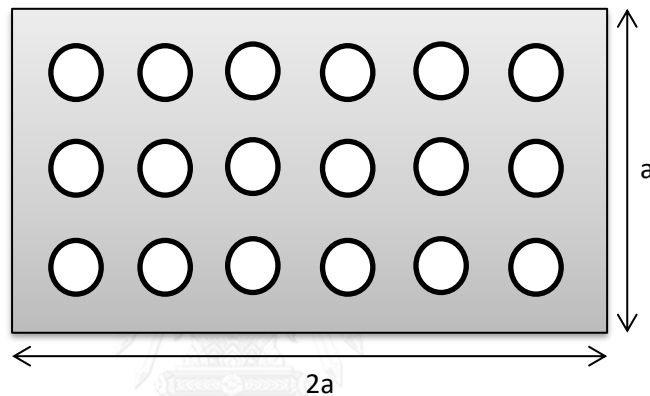


Figure 18 Fully longitudinal porous dielectric-loaded rectangular waveguide with  $\epsilon_r = 2.25$  and  $FF = 0.28$

Figure 17 and 18 show one case amongst several cases of comparison between fully dielectric-loaded rectangular waveguide and fully porous dielectric-loaded rectangular waveguide. The normalized phase constant  $\beta/k_0$  of the first and second guiding modes of waveguide structure as shown in Figure 18 are almost equal to normalized phase constant that generated from dispersion relation of closed-form solution of waveguide structure as shown in Figure 17. As we know that waveguide in Figure 18 is the rectangular waveguide fully loaded by dielectric material with  $\epsilon_r = 2.25$  and air-tube with  $FF = 0.28$ . So, this waveguide can be equivalent to waveguide structure as in Figure 17. Table 1 and Table 2 show the comparison of normalized phase constant  $\beta/k_0$  versus some discrete values  $k_0a$ . The differences values in percentage is around 1%. This comparison values can lead to the assumption of the equivalent of these two waveguides.

Table 1 Comparison of some discrete values of first guiding mode between fully dielectric-loaded rectangular waveguide with  $\epsilon_r = 1.86$  and fully porous dielectric-loaded rectangular waveguide with  $\epsilon_r = 2.25$  and  $FF = 0.28$

$\epsilon_r = 1.86$ Fully loaded in RWG			$\epsilon_r = 2.25$ with $FF=0.28$ fully loaded in RWG		Differences (%)
$\epsilon_r$	$k_0 a$	$\beta / k_0$ mode 1	$k_0 a$	$\beta / k_0$ mode 1	
1.86	1.16	0.167862338	1.16	0.168299532	0.260447571
1.86	1.17	0.243633224	1.17	0.244140897	0.20837571
1.86	1.18	0.299578369	1.18	0.300155713	0.192718776
1.86	1.19	0.345505916	1.19	0.346146281	0.185341334
1.86	1.2	0.385050502	1.2	0.385748052	0.181158213
1.86	1.3	0.633623934	1.3	0.634723322	0.173507903
1.86	1.4	0.776143002	1.4	0.777507825	0.175846911
1.86	1.5	0.874350553	1.5	0.875923356	0.179882419
1.86	1.6	0.9471792	1.6	0.94892876	0.18471265
1.86	1.7	1.003540445	1.7	1.005448109	0.190093347
1.86	1.8	1.048440935	1.8	1.050495157	0.195931078
1.86	1.9	1.0849895	1.9	1.08718316	0.202182533
1.86	2	1.115246609	2	1.117575523	0.208825005
1.86	2.1	1.140642696	2.1	1.143104722	0.215845538
1.86	2.2	1.162206152	2.2	1.164800618	0.223236285
1.86	2.3	1.180696984	2.3	1.183424303	0.230992291
1.86	2.31	1.182400472	2.31	1.185141132	0.231787845
1.86	2.32	1.184079576	2.32	1.186833591	0.232587017
1.86	2.33	1.185734774	2.33	1.188502158	0.233389803

1.8 6	2.34	1.187366534	2.34	1.190147302	0.234196202
1.8 6	2.35	1.188975311	2.35	1.191769477	0.235006211
1.8 6	2.36	1.190561548	2.36	1.193369128	0.235819828
1.8 6	2.37	1.192125678	2.37	1.194946689	0.236637051
1.8 6	2.38	1.193668122	2.38	1.196502581	0.237457877
1.8 6	2.39	1.195189292	2.39	1.198037216	0.238282306
1.8 6	2.4	1.196689589	2.4	1.199550997	0.239110335
1.8 6	2.5	1.210626284	2.5	1.213623653	0.247588301
1.8 6	2.6	1.222853148	2.6	1.225988847	0.256424794
1.8 6	2.7	1.233644717	2.7	1.23692151	0.265618913
1.8 6	2.8	1.243221416	2.8	1.24664239	0.275170111
1.8 6	2.9	1.251762135	2.9	1.255330634	0.285078091
1.8 6	3	1.259413444	3	1.26313303	0.295342745

Just note that the value  $\beta/k_0$  of the first and second guiding mode of waveguide structure in Figure 17 can be computed from the dispersion relation for  $TE_{10}$  and  $TE_{01}$  of closed-form solution as:

$$\text{In mode 1 (First guiding mode } TE_{10}\text{): } \beta/k_0 = \sqrt{\varepsilon_r - \left(\frac{\pi}{2k_0a}\right)^2} \quad (4.2.1)$$

$$\text{In mode 2 (Second guiding mode } TE_{01}\text{): } \beta/k_0 = \sqrt{\varepsilon_r - \left(\frac{\pi}{k_0a}\right)^2} \quad (4.2.2)$$

The differences (%) are calculated by the formula:

$$\text{differences(\%)} = \frac{|\beta/k_0 \text{ simulate} - \beta/k_0 \text{ closed form}| \times 100}{\beta/k_0 \text{ closed form}} \quad (4.2.3)$$

Where  $\beta/k_0 \text{ simulate}$  are taken from the normalized phase constant of waveguide in Figure 4-11.  $\beta/k_0 \text{ closed form}$  are taken from the normalized phase constant of waveguide in Figure 4-10.

Table 2 Comparison of some discrete values of second guiding mode between fully dielectric-loaded rectangular waveguide with  $\epsilon_r = 1.86$  and fully porous dielectric-loaded rectangular waveguide with  $\epsilon_r = 2.25$  and  $FF = 0.28$

$\epsilon_r = 1.86$ Fully loaded in RWG			$\epsilon_r = 2.25$ with $FF=0.28$ fully loaded in RWG		Differences (%)
	$k_0 a$	$\beta / k_0$ mode 2	$k_0 a$	$\beta / k_0$ mode 2	
1.86	2.31	0.110830966	2.31	0.119128017	7.486221185
1.86	2.32	0.167862338	2.32	0.173874061	3.581341009
1.86	2.33	0.209446457	2.33	0.214633088	2.476351596
1.86	2.34	0.243633224	2.34	0.24839588	1.954846339
1.86	2.35	0.273219989	2.35	0.277732019	1.651427403
1.86	2.36	0.299578369	2.36	0.303931584	1.453113974
1.86	2.37	0.323503516	2.37	0.327752656	1.313475751
1.86	2.38	0.345505916	2.38	0.348097343	0.750038364
1.86	2.39	0.365936839	2.39	0.370072427	1.130136864
1.86	2.4	0.385050502	2.4	0.389158381	1.066841625
1.86	2.5	0.531473424	2.5	0.535677506	0.791023984
1.86	2.6	0.633623934	2.6	0.63810418	0.707082794
1.86	2.7	0.712402377	2.7	0.717179995	0.670634732
1.86	2.8	0.776143002	2.8	0.78121345	0.653287828
1.86	2.9	0.82923686	2.9	0.834200619	0.598593682
1.86	3	0.874350553	3	0.879978697	0.643694284

Several pairs of simulation model of equivalent waveguide are constructed, computed, and simulated to find the value of differences (%). Finally, we can build

table that show us the pair values of filling factor  $FF$  and its equivalent effective relative permittivity.

## CHAPTER V CHARACTERIZATION OF EFFECTIVE RELATIVE PERMITTIVITY OF POROUS DIELECTRIC

In this section, our goal is to characterize the behavior of effective relative permittivity of the porous dielectric material. As we already know in chapter 4, the composite material of dielectric and air-holes can be considered as one pure material with value of effective relative permittivity between 1 and the relative permittivity of the background material.

In this chapter, we will use the dispersion relation of the first guiding mode of rectangular waveguide that is derived from the closed-form solution. This relation will be used to calculate the equivalent effective relative permittivity from known result of simulation in each case.

The formula that we use to calculate effective permittivity is written as:

$$\varepsilon_{eff} = \left( (\beta / k_0)_{FEM} \right)^2 + \left( \frac{\pi}{2(k_0 a)_{FEM}} \right)^2 \quad (5.1)$$

Where  $\beta / k_0$  and  $k_0 a$  are pair of simulation results with various filling factor (FF). Several cases of filling factor from two different value of relative permittivity of background material are used to find the variation of effective permittivity of the composite material.

### 5.1. Case of background material with $\varepsilon_r = 2.25$

In this case, we use porous structure as circular holes from FF=0 to FF=0.6 and we use square holes from FF=0.7 to FF=0.9. The results of variation of effective relative permittivity depend on frequency in each case of FF are shown as follow.

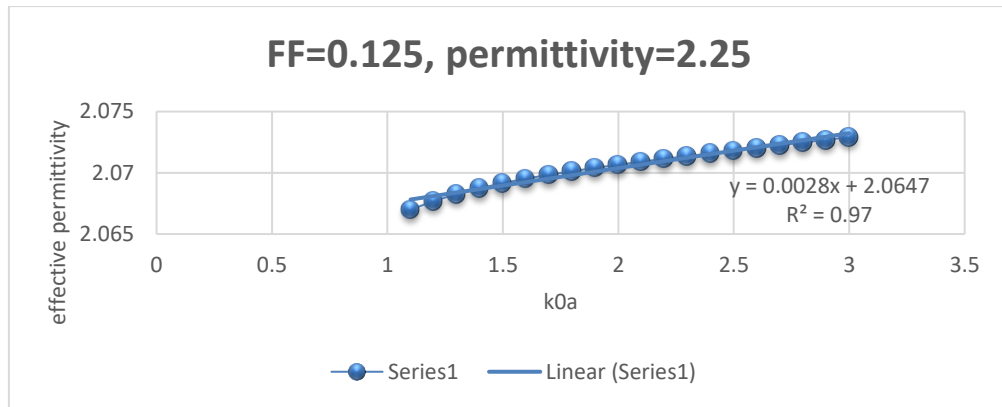


Figure 19 Effective permittivity versus frequency for FF=0.125

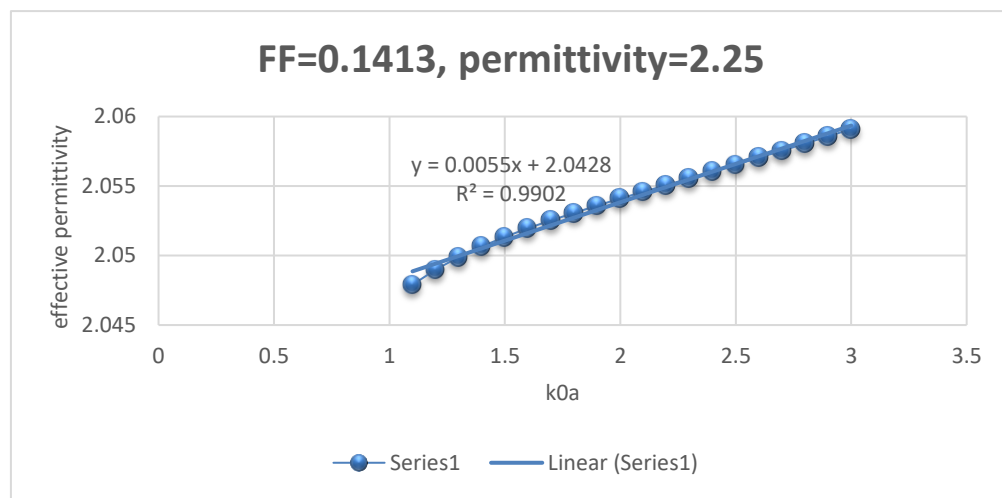


Figure 20 Effective permittivity versus frequency for FF=0.1413

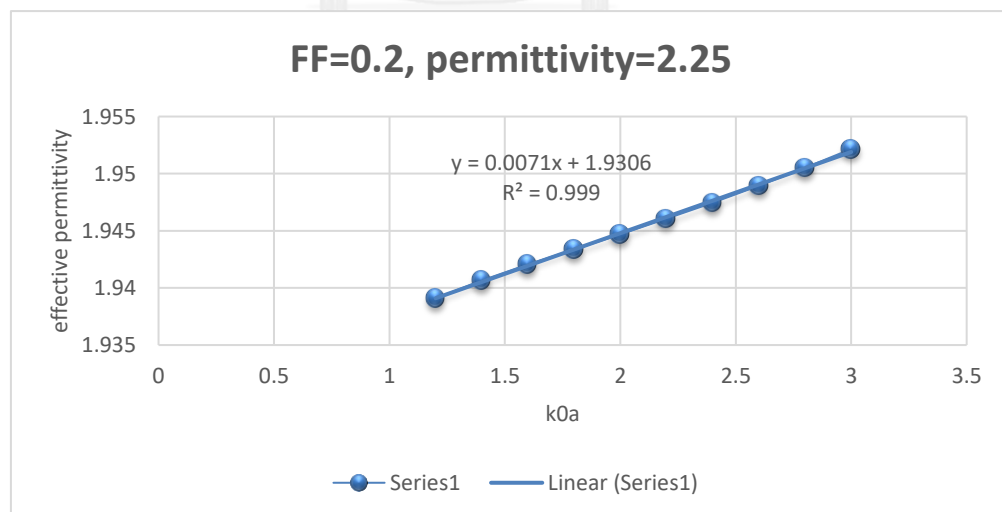


Figure 21 Effective permittivity versus frequency for FF=0.2

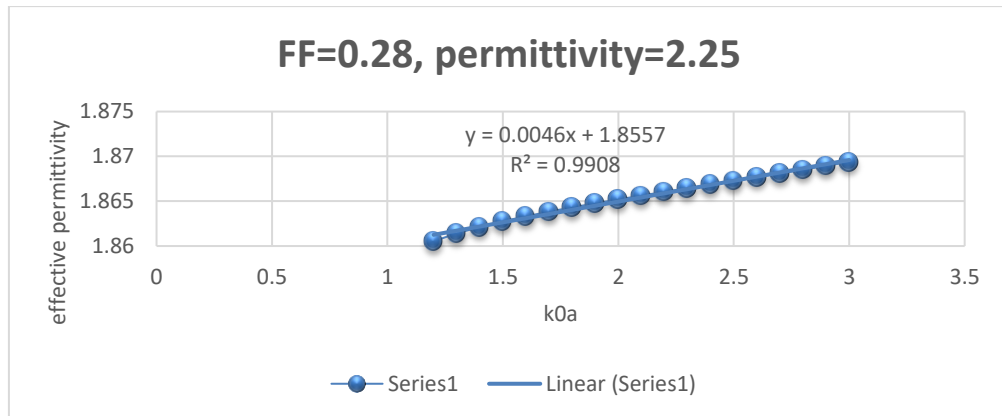


Figure 22 Effective permittivity versus frequency for FF=0.28

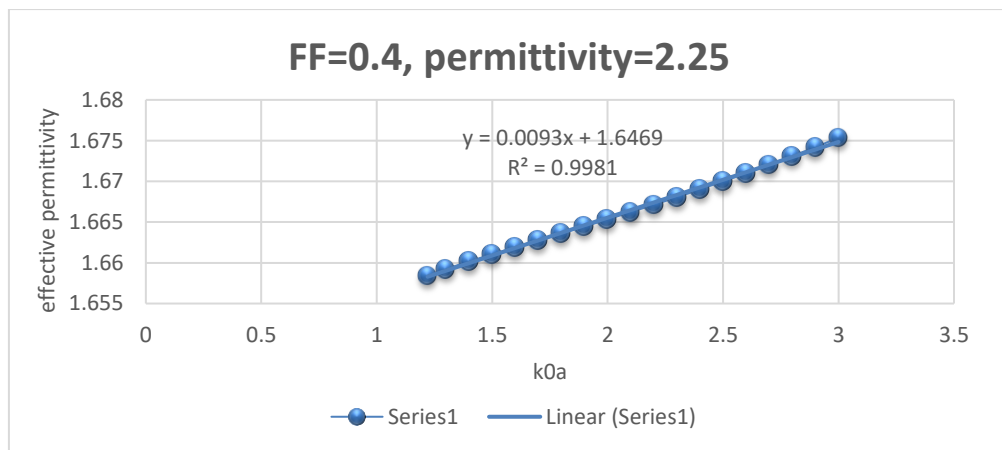


Figure 23 Effective permittivity versus frequency for FF=0.4

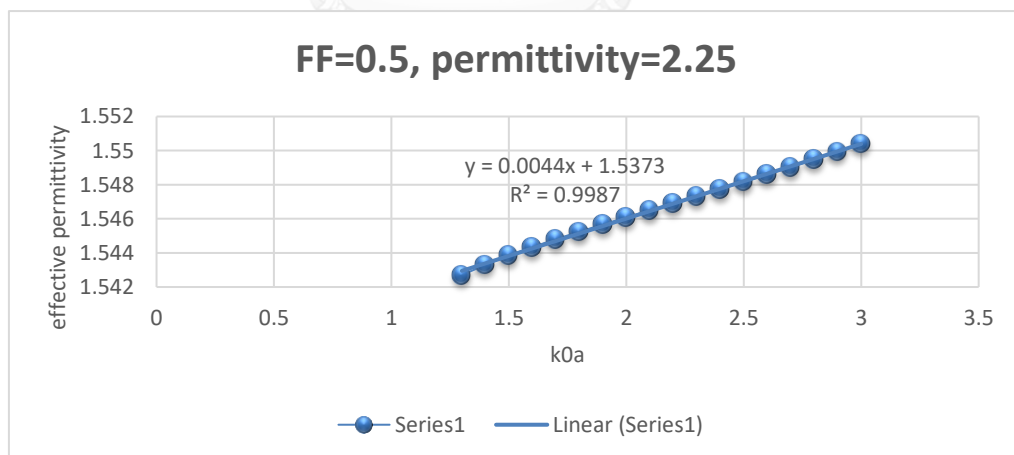


Figure 24 Effective permittivity versus frequency for FF=0.5

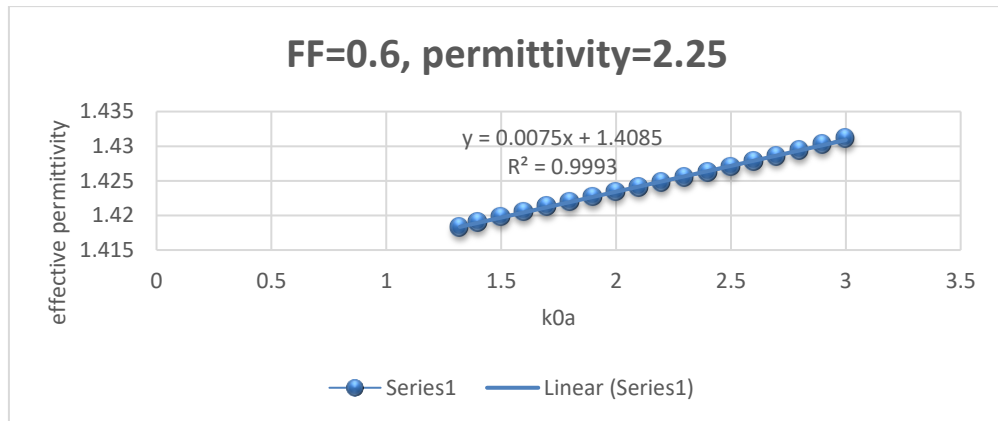


Figure 25 Effective permittivity versus frequency for FF=0.6

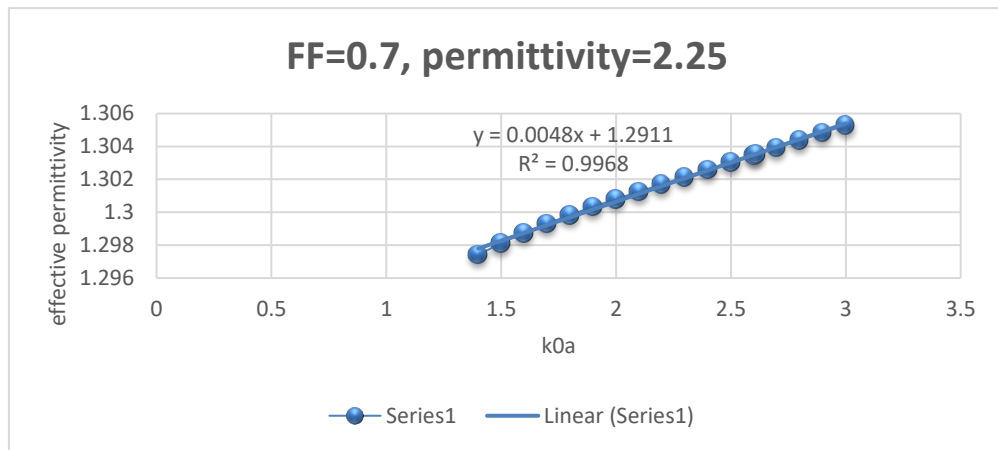


Figure 26 Effective permittivity versus frequency for FF=0.7

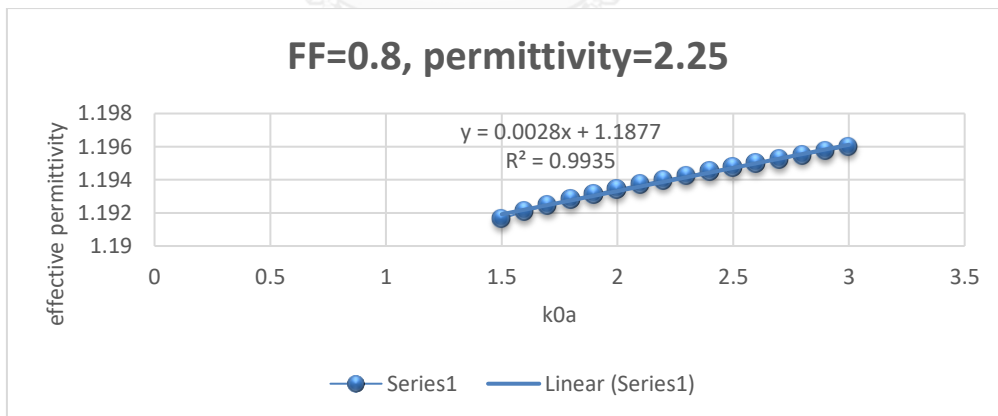


Figure 27 Effective permittivity versus frequency for FF=0.8

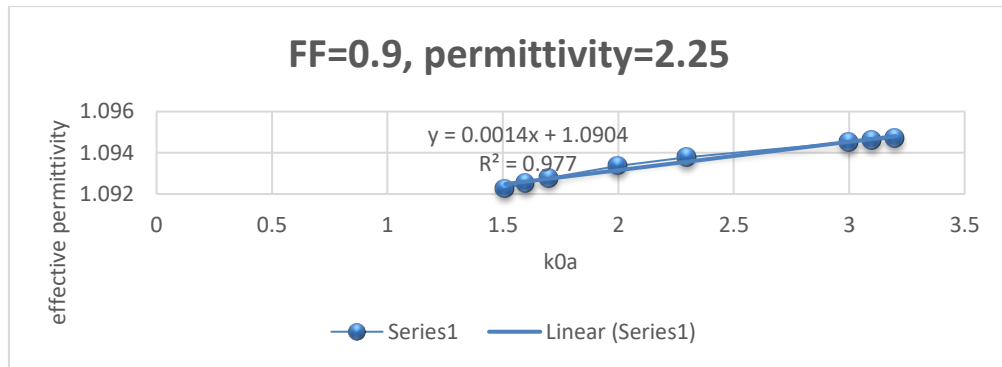


Figure 28 Effective permittivity versus frequency for FF=0.9

By using the fit line in each case of filling factor, we can see the rate of change of effective relative permittivity  $\epsilon_{eff}$  versus value of  $k_0a$ . All of rates of change in these cases are very small that can be assumed as no change in the case of background material with  $\epsilon_r = 2.25$ . Figure 19 to Figure 28 show that the value of effective relative permittivity has no significant change over the single-bandwidth frequency range.

Table 3 Average value of effective relative permittivity versus FF for background material  $\epsilon_r = 2.25$

$\epsilon_r = 2.25$	
FF	Average $\epsilon_{eff}$
0	2.25
0.125	2.06925548
0.1413	2.05254112
0.2	1.9429004
0.28	1.86297021
0.4	1.662908
0.5	1.54554314
0.6	1.42211922
0.7	1.30139683
0.8	1.1938012
0.9	1.09291894
1	1

We choose the average value of effective relative permittivity over the frequency range of single-mode bandwidth in each case of FF. Average value of effective relative permittivity in each case are calculated and shown in Table 3 below in the case of background material  $\epsilon_r = 2.25$ .

We can see that plot of Average effective permittivity versus FF almost fit to the line with line's equation  $\epsilon_{eff} = (1 - \epsilon_r)FF + \epsilon_r$  for  $\epsilon_r = 2.25$ . We can assume that the Average effective relative permittivity of the composite material between dielectric material and air-holes has the linear relationship with filling factor FF.

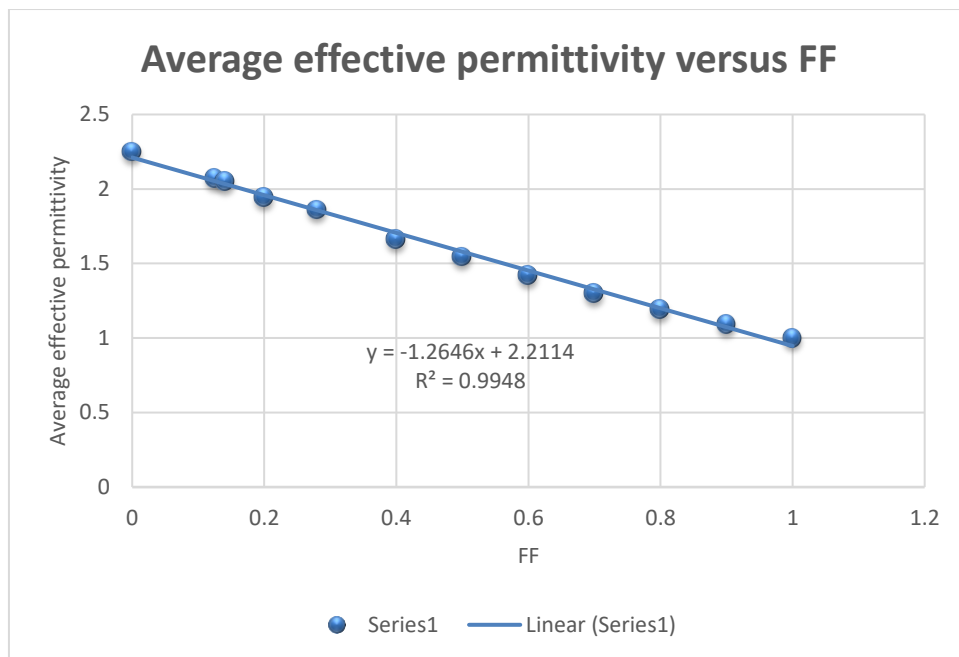


Figure 29 Graph of average effective relative permittivity versus FF and its fit line for background material  $\epsilon_r = 2.25$  by the sample of FF from 0.1 to 0.9

This fit line can also be found by using only in the case of circular air-tube of FF=0.6. The sample data and fit line is plot together as shown in Figure 29.

## 5.2. Case of background material with $\epsilon_r = 3.2$

In order to get more data to assume the relationship between effective relative permittivity of the composite material and filling factor of drilling air-tubes, we simulate more proposed model of waveguide with variation of filling factor from 0.1 to 0.6 as above. The differences in simulation are the value of background material  $\epsilon_r = 3.2$  (material type: Silicon rubber).

In these simulations, we create several models of fully porous dielectric-loaded rectangular waveguide with different filling factor of air-tubes in the background material with relative permittivity  $\epsilon_r = 3.2$ .

In this case, we use porous structure as circular holes from FF=0 to FF=0.6. The results of variation of effective relative permittivity depend on frequency in each case of FF are shown as follow.

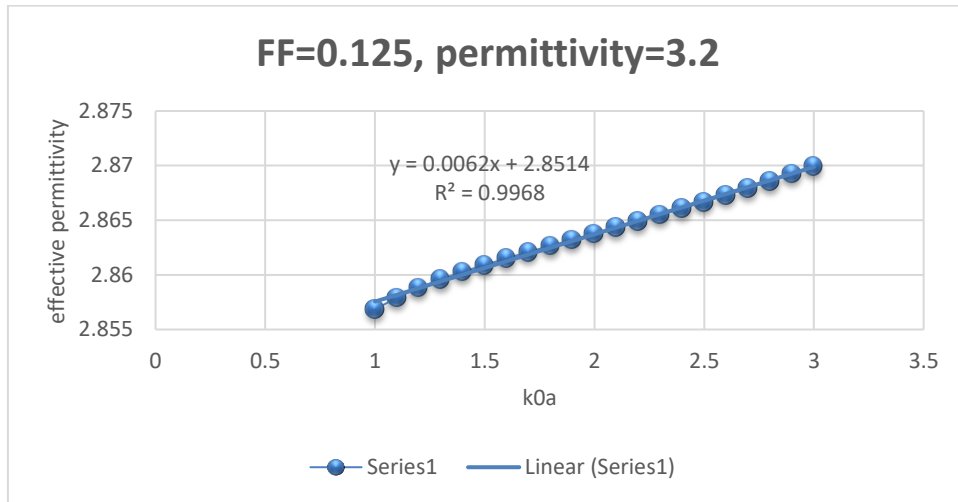


Figure 30 Effective permittivity versus frequency for background material  $\epsilon_r = 3.2$  in the case of FF=0.125

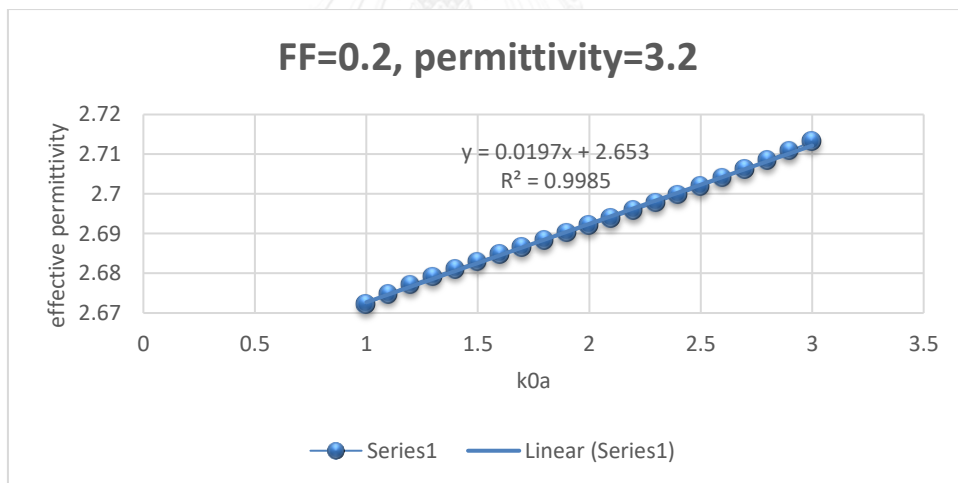


Figure 31 Effective permittivity versus frequency for background material  $\epsilon_r = 3.2$  in the case of FF=0.2

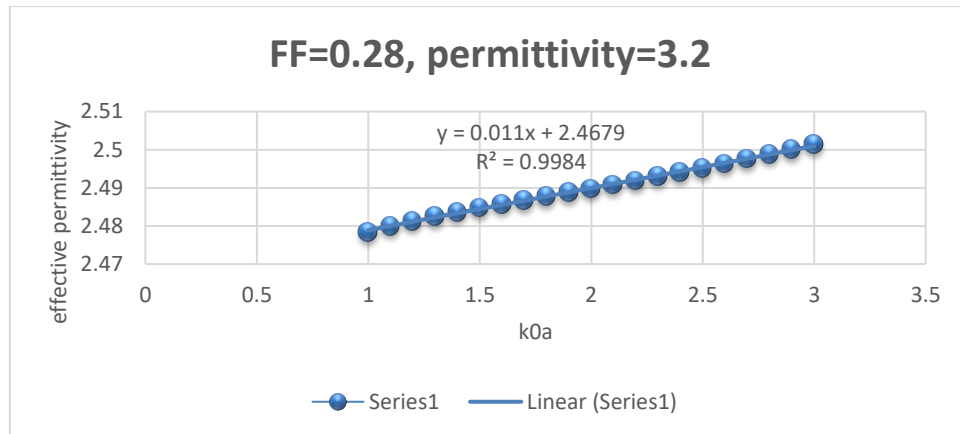


Figure 32 Effective permittivity versus frequency for background material in the case of FF=0.28

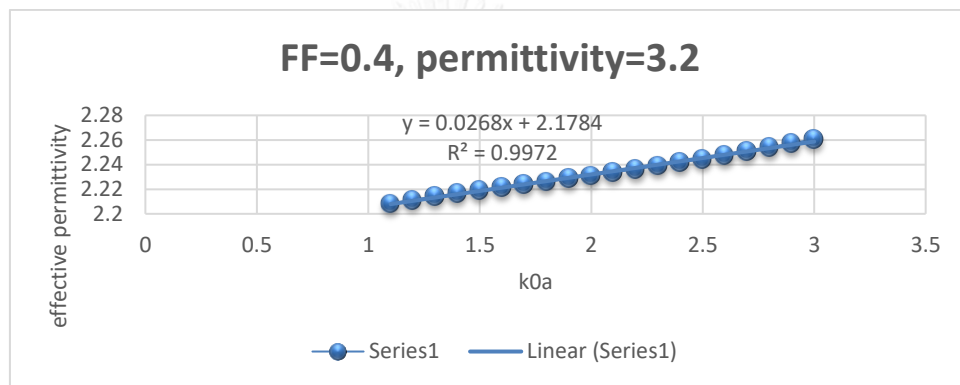


Figure 33 Effective permittivity versus frequency for background material  $\epsilon_r = 3.2$  in the case of FF=0.4

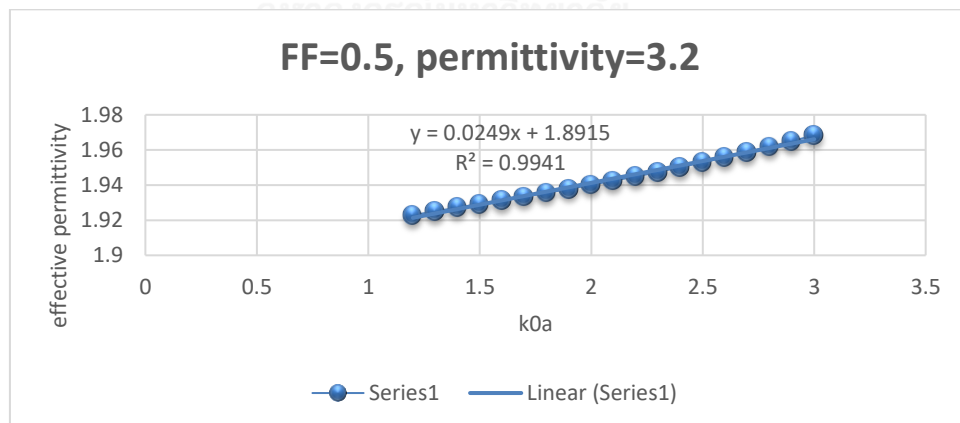


Figure 34 Effective permittivity versus frequency for background material  $\epsilon_r = 3.2$  in the case of FF=0.5

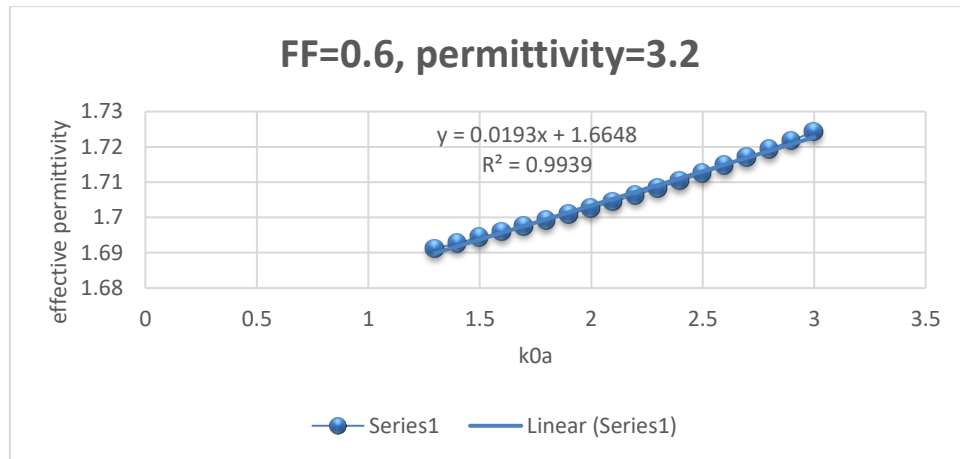


Figure 35 Effective permittivity versus frequency for background material

$\epsilon_r = 3.2$  in the case of FF=0.6

By using the fit line in each case of filling factor, we can see the rate of change of effective relative permittivity  $\epsilon_{eff}$  versus value of  $k_0a$ . All of rates of change in these cases are very small that can be assumed as small change in the case of background material with  $\epsilon_r = 3.2$ .

Average value of effective relative permittivity in each case are also calculate and shown in Table 4 in the case of background material  $\epsilon_r = 3.2$ .

Table 4 Average effective relative permittivity versus filling factor FF for background material  $\epsilon_r = 3.2$

$\epsilon_r = 3.2$	
FF	Average $\epsilon_{eff}$
0	3.2
0.125	2.859669
0.2	2.680779
0.28	2.483964
0.4	2.22009
0.5	1.932669
0.6	1.69955
1	1

We can see the fit line of this almost equal to  $\epsilon_{eff} = (1 - \epsilon_r)FF + \epsilon_r$  with  $\epsilon_r = 3.2$ .

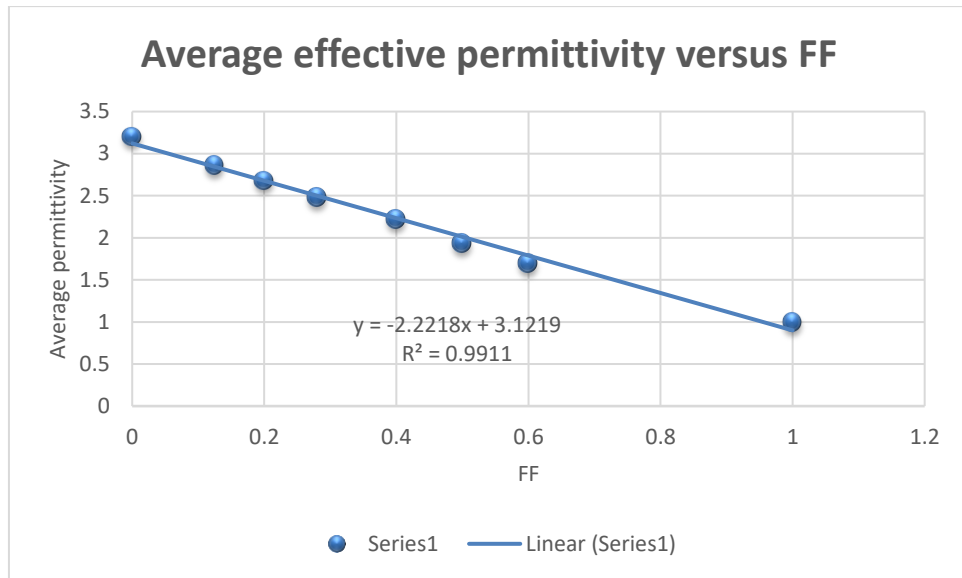


Figure 36 Graph of average effective relative permittivity versus FF and its fit line for background material  $\epsilon_r = 3.2$  by the sample of FF from 0.1 to 0.6

From these two cases of different background materials, we see that the rate of change of  $\epsilon_{eff}$  become significant when the relative permittivity of background material become higher.

But these rates of change are acceptable because they are so small. Anyway, the highest bandwidth of waveguide has value  $\frac{\pi}{2}$ . If we multiply the rate of change with bandwidth, we see that they are acceptable for single-mode operation by using average value of  $\epsilon_{eff}$ .

## CHAPTER VI APPLICATION AND OPTIMIZING TOPOLOGY OF POROUS DIELECTRIC MATERIAL

### 6.1. Application with half porous dielectric-loaded rectangular waveguide

The relation between filling factor and effective permittivity are verified not only in fully porous dielectric-loaded rectangular waveguide but also in partially porous dielectric-loaded rectangular waveguide such as half porous dielectric-loaded rectangular waveguide. Five different cases of waveguide's pairs are constructed for simulation and comparison. In these five cases, three case are chosen for FF=0.5, FF=0.28 and FF=0.125.

The fourth case is chosen at FF=0.4 for background material  $\epsilon_r = 2.25$ . The fifth case is chosen with FF=0.8 that is the case of high value of filling factors.

**Case 1: Relative permittivity 1.545543 and relative permittivity 2.25 with FF=0.5**

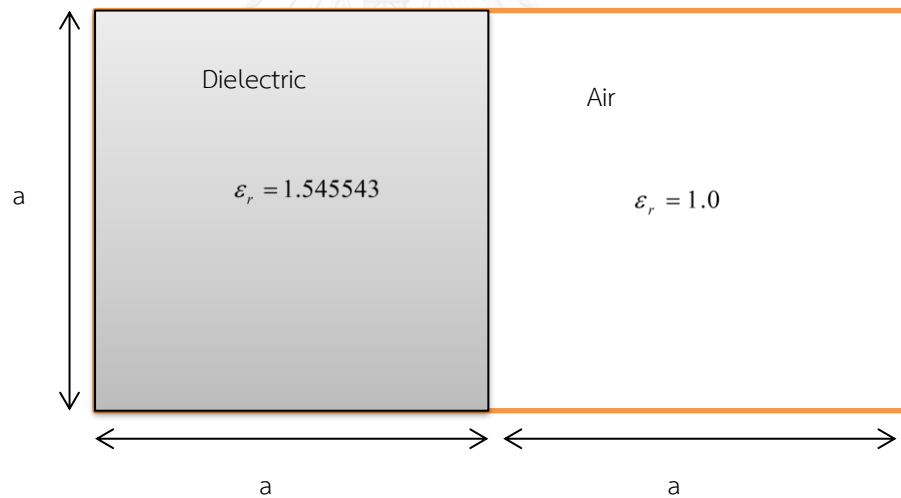


Figure 37 Half dielectric-loaded rectangular waveguide with  $\epsilon_r = 1.545543$

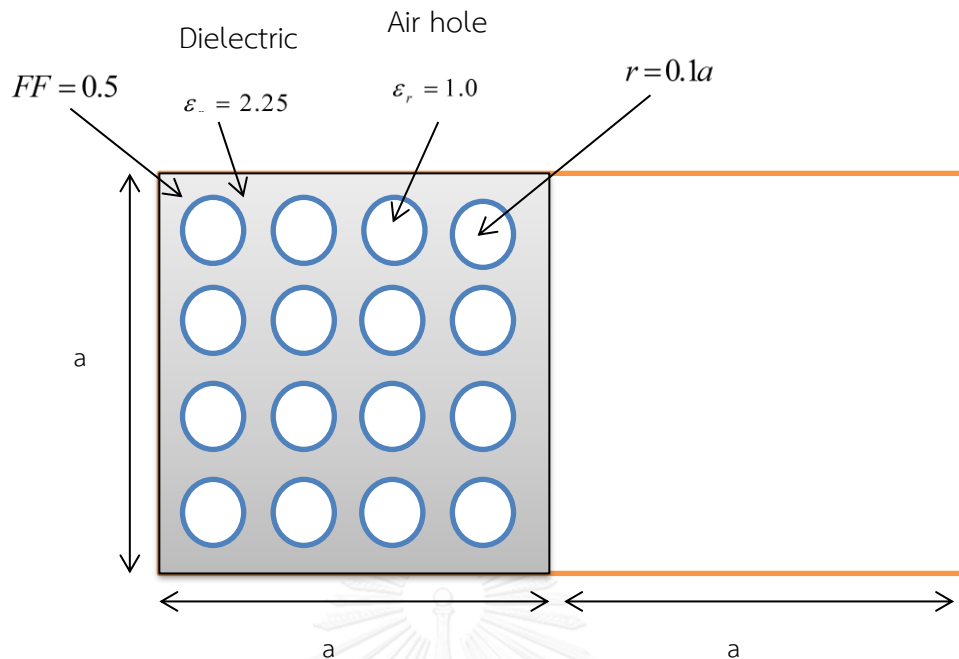


Figure 38 Half porous dielectric-loaded rectangular waveguide with  $\epsilon_r = 2.25$  and  $FF = 0.5$

In this case, the rectangular waveguide half loaded by dielectric material with relative permittivity  $\epsilon_r = 1.545522$  are compared with rectangular waveguide half loaded by composite material of dielectric material with relative permittivity  $\epsilon_r = 2.25$  and air-tube by  $FF = 0.5$ . The parameters and structure of waveguide for simulation are shown in figure 37 and 38. Table 6 and Table 7 show the results of simulation and comparison of the normalized phase constant  $\beta/k_0$ .

Table 5 Comparison of some discrete values of first guiding mode between Half dielectric-loaded rectangular waveguide with  $\epsilon_r = 1.545543$  and fully porous dielectric-loaded rectangular waveguide with  $\epsilon_r = 2.25$  and  $FF = 0.5$  for 16 circular holes

Half dielectric-Loaded RWG		Half porous dielectric-loaded RWG		Error (%) of $\beta/k_0$
$\epsilon_r = 1.545543$		$\epsilon_r = 2.25$ , $FF=0.5$ , 16 circular holes		
$k_0a$	$\beta/k_0$ mode 1	$k_0a$	$\beta/k_0$ mode 1	
1.4	0.169157933	1.4	0.171231031	1.225539755
1.5	0.439735519	1.5	0.440641545	0.206038863
1.6	0.573360213	1.6	0.574106711	0.130197032
1.7	0.664434358	1.7	0.665103887	0.100766655

1.8	0.732445931	1.8	0.733062966	0.084243106
1.9	0.785754682	1.9	0.786329429	0.073145946
2	0.828877252	2	0.829415036	0.064881013
2.1	0.864568649	2.1	0.865072928	0.058327214
2.2	0.894641269	2.2	0.895114841	0.05293421
2.3	0.920350881	2.3	0.920796433	0.04841114
2.4	0.942601256	2.4	0.943021646	0.044598936
2.5	0.962062047	2.5	0.962460446	0.041410991
2.6	0.979241035	2.6	0.979621007	0.038802794
2.7	0.994530575	2.7	0.994896116	0.03675512

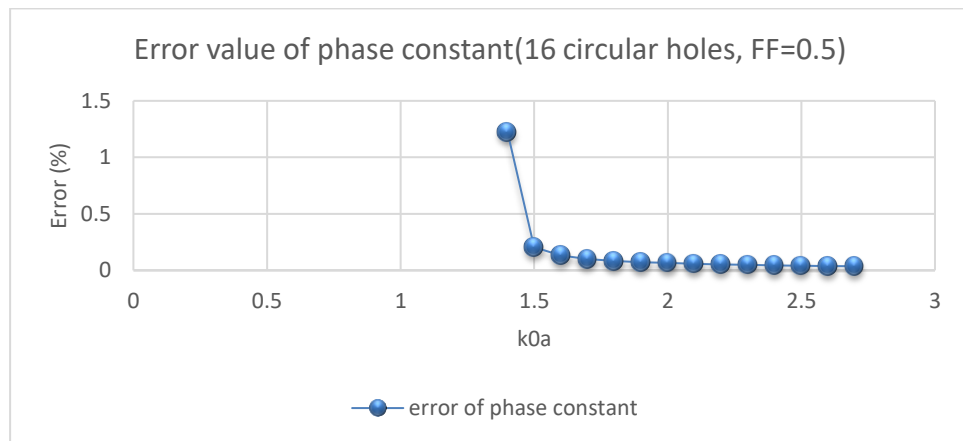


Figure 39 Plot of error of  $\beta/k_0$  versus  $k_0a$  for 16 circular holes with  $FF=0.5$

Table 6 Comparison of some discrete values of first guiding mode between Half dielectric-loaded rectangular waveguide with  $\epsilon_r = 1.545543$  and fully porous dielectric-loaded rectangular waveguide with  $\epsilon_r = 2.25$  and  $FF = 0.5$  for 9 square holes

Half dielectric-Loaded RWG		Half porous dielectric-loaded RWG		Error (%) of $\beta/k_0$
$\epsilon_r = 1.545543$		$\epsilon_r = 2.25$ , $FF=0.5$ , 9 square holes		
$k_0a$	$\beta/k_0$ mode 1	$k_0a$	$\beta/k_0$ mode 1	
1.4	0.169157933	1.4	0.165404134	2.219109181
1.5	0.439735519	1.5	0.438235488	0.341121266
1.6	0.573360213	1.6	0.572097121	0.220296524
1.7	0.664434358	1.7	0.663203872	0.185193043
1.8	0.732445931	1.8	0.731169313	0.174295173
1.9	0.785754682	1.9	0.784389072	0.173795929
2	0.828877252	2	0.827395052	0.178820214
2.1	0.864568649	2.1	0.862950388	0.187175539
2.2	0.894641269	2.2	0.892872545	0.197702046

2.3	0.920350881	2.3	0.918420864	0.209704475
2.4	0.942601256	2.4	0.940501892	0.22272026
2.5	0.962062047	2.5	0.959787608	0.236412937
2.6	0.979241035	2.6	0.976787852	0.250518808
2.7	0.994530575	2.7	0.991896873	0.264818608

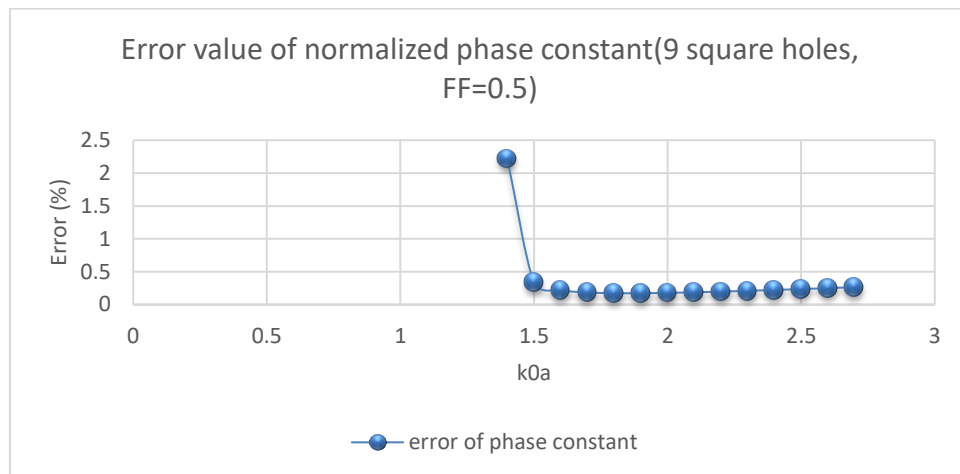


Figure 40 Plot of error of  $\beta/k_0$  versus  $k_0a$  for 9 square holes with FF=0.5  
Case 2: Relative permittivity 1.86297 and relative permittivity 2.25 with FF=0.28

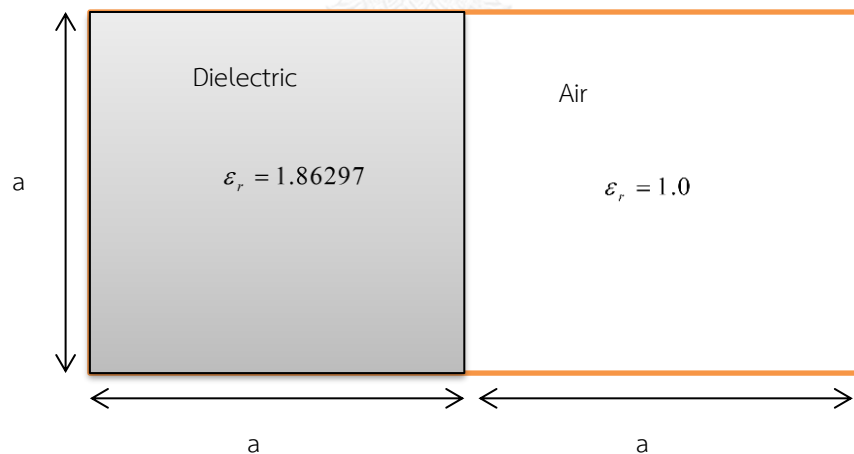


Figure 41 Half dielectric-loaded rectangular waveguide with  $\epsilon_r = 1.86297$

In this case, the rectangular waveguide half loaded by dielectric material with relative permittivity  $\epsilon_r = 1.86297$  are compared with rectangular waveguide half loaded by composite material of dielectric material with relative permittivity  $\epsilon_r = 2.25$  and air-tube by  $FF = 0.28$ . The parameters and structure of waveguide for

simulation are shown in figure 41 and 42. Table 8 and 9 show the results of simulation and comparison of the normalized phase constant  $\beta/k_0$ .

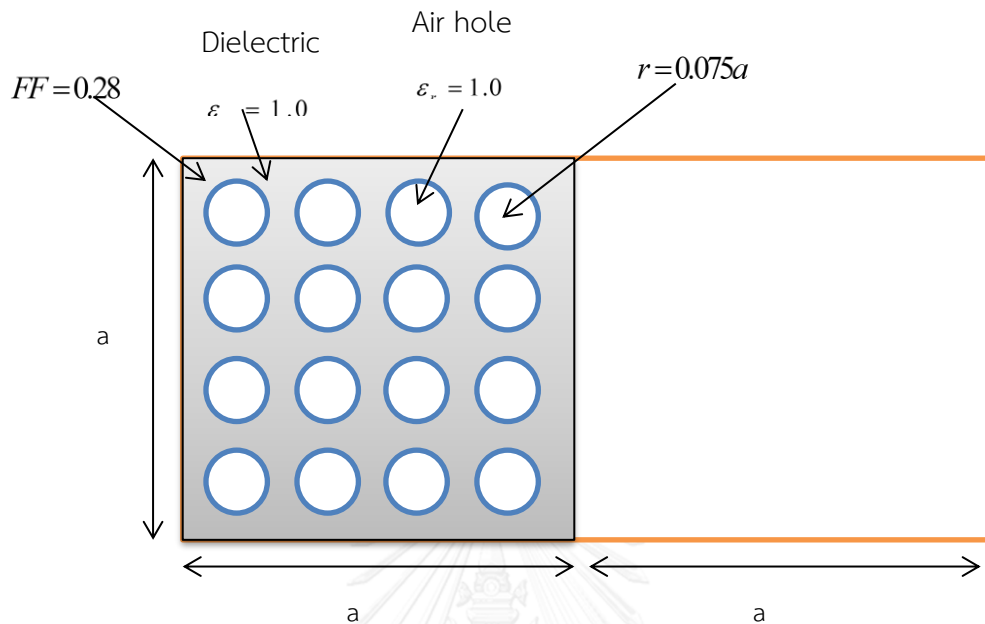


Figure 42 Half porous dielectric-loaded rectangular waveguide with  $\epsilon_r = 2.25$  and  $FF = 0.28$

Table 7 Comparison of some discrete values of first guiding mode between Half dielectric-loaded rectangular waveguide with  $\epsilon_r = 1.86297$  and fully porous dielectric-loaded rectangular waveguide with  $\epsilon_r = 2.25$  and  $FF = 0.28$  for 16 circular holes

Half dielectric-Loaded RWG		Half porous dielectric-loaded RWG		Error (%) of $\beta/k_0$
$\epsilon_r = 1.86297$		$\epsilon_r = 2.25, FF=0.28, 16$ circular holes		
$k_0 a$	$\beta/k_0$ mode 1	$k_0 a$	$\beta/k_0$ mode 1	
1.3	0.055324117	1.3	0.04751	14.12437721
1.4	0.457808214	1.4	0.457034	0.169074057
1.5	0.614415054	1.5	0.613869	0.088912406
1.6	0.718488277	1.6	0.718016	0.065729917
1.7	0.795279201	1.7	0.794826	0.05692533
1.8	0.855066293	1.8	0.854606	0.053842374
1.9	0.903256968	1.9	0.902773	0.053538606
2	0.943090201	2	0.942574	0.054710744
2.1	0.976666141	2.1	0.976113	0.056672478

2.2	1.005421641	2.2	1.004828	0.059013943
2.3	1.030378791	2.3	1.029745	0.061466254
2.4	1.052286523	2.4	1.051615	0.063840644
2.5	1.071706652	2.5	1.070999	0.065998582

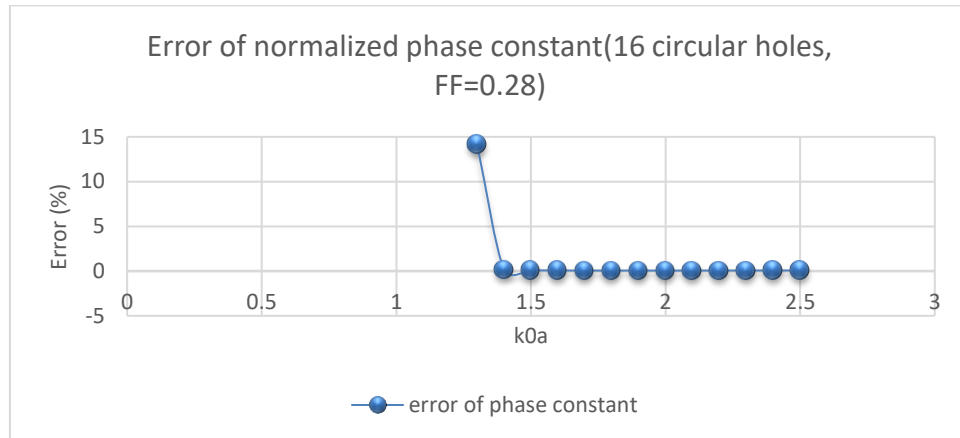


Figure 43 Plot of error of  $\beta/k_0$  versus  $k_0a$  for 16 circular holes with  $FF=0.28$

Table 8 Comparison of some discrete values of first guiding mode between Half dielectric-loaded rectangular waveguide with  $\epsilon_r = 1.86297$  and fully porous dielectric-loaded rectangular waveguide with  $\epsilon_r = 2.25$  and  $FF = 0.28$  for 9 square holes

Half dielectric-Loaded RWG		Half porous dielectric-loaded RWG		Error (%) of $\beta/k_0$
$\epsilon_r = 1.86297$		$\epsilon_r = 2.25, FF=0.28, 9$ square holes		
$k_0a$	$\beta/k_0$ mode 1	$k_0a$	$\beta/k_0$ mode 1	
1.4	0.457808214	1.4	0.435561	4.859503651
1.5	0.614415054	1.5	0.597938	2.681825949
1.6	0.718488277	1.6	0.704304	1.974234099
1.7	0.795279201	1.7	0.782306	1.631287777
1.8	0.855066293	1.8	0.842809	1.433475675
1.9	0.903256968	1.9	0.891445	1.307736041
2	0.943090201	2	0.931559	1.222707084
2.1	0.976666141	2.1	0.965311	1.162635213
2.2	1.005421641	2.2	0.994174	1.118699111
2.3	1.030378791	2.3	1.019194	1.085547262
2.4	1.052286523	2.4	1.041135	1.059728259
2.5	1.071706652	2.5	1.060573	1.038908438

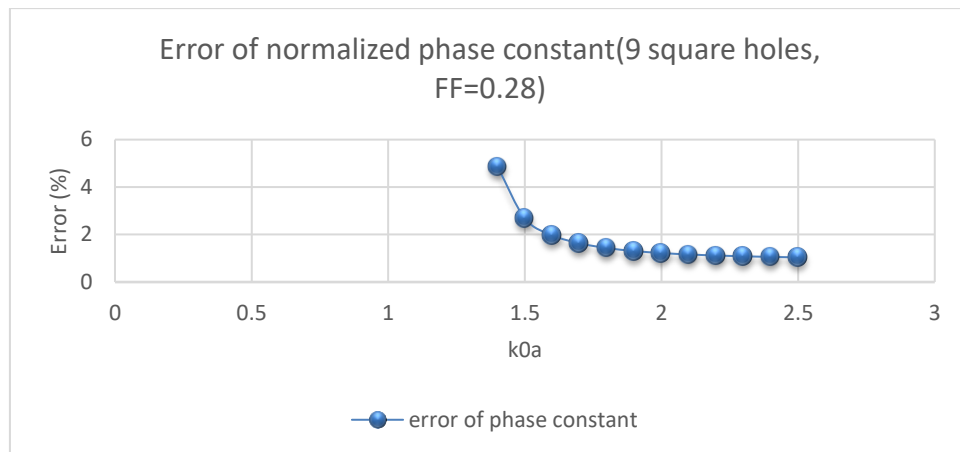


Figure 44 Plot of error of  $\beta/k_0$  versus  $k_0a$  for 9 square holes with  $FF=0.28$

Case 3: Relative permittivity 2.069255 and relative permittivity 2.25 with  $FF=0.125$

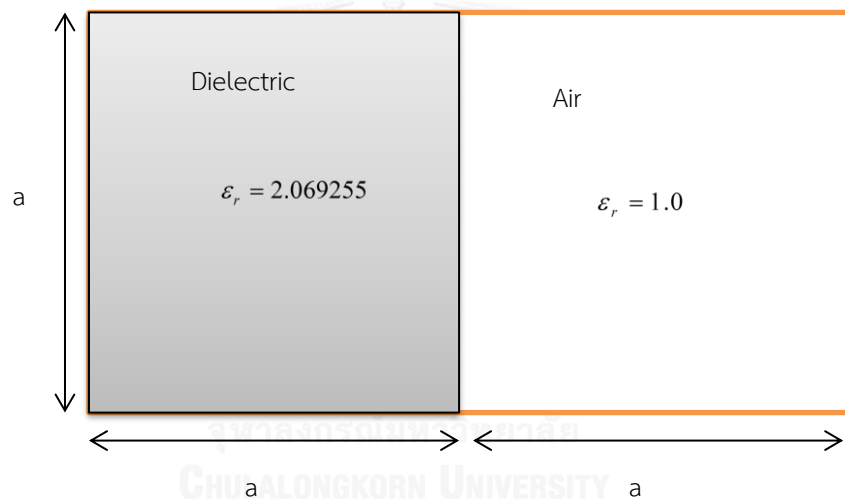


Figure 45 Half dielectric-loaded rectangular waveguide with  $\epsilon_r = 2.069255$

In this case the rectangular waveguide half loaded by dielectric material with relative permittivity  $\epsilon_r = 2.069255$  are compared with rectangular waveguide half loaded by composite material of dielectric material with relative permittivity  $\epsilon_r = 2.25$  and air-tube by  $FF = 0.125$ . The parameters and structure of waveguide for simulation are shown in figure 45 and 46. Table 10 and 11 show the results of simulation and comparison of the normalized phase constant  $\beta/k_0$ .

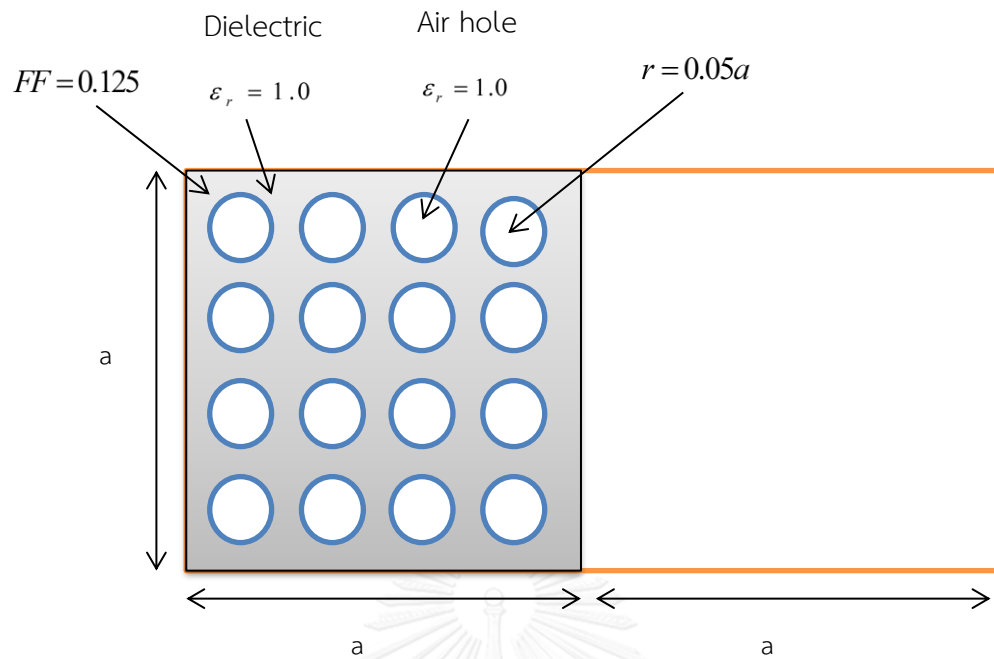


Figure 46 Half porous dielectric-loaded rectangular waveguide with  $\epsilon_r = 2.25$  and  $FF = 0.125$

Table 9 Comparison of some discrete values of first guiding mode between Half dielectric-loaded rectangular waveguide with  $\epsilon_r = 2.069255$  and fully porous dielectric-loaded rectangular waveguide with  $\epsilon_r = 2.25$  and  $FF = 0.125$  for 16 circular holes

Half dielectric-Loaded RWG		Half porous dielectric-loaded RWG		Error (%) of $\beta / k_0$
$\epsilon_r = 2.069255$		$\epsilon_r = 2.25, FF=0.125, 16$ circular holes		
$k_0 a$	$\beta / k_0$ mode 1	$k_0 a$	$\beta / k_0$ mode 1	
1.3	0.351007703	1.3	0.351846022	0.238831984
1.4	0.576474303	1.4	0.577003272	0.091759333
1.5	0.709206817	1.5	0.709610208	0.05687917
1.6	0.802843396	1.6	0.803147551	0.037884824
1.7	0.873942679	1.7	0.874153367	0.024107751
1.8	0.930328049	1.8	0.930446084	0.012687475
1.9	0.976410898	1.9	0.97643597	0.002567749
2	1.014939314	2	1.014871245	0.0067067
2.1	1.047739042	2.1	1.047578259	0.015345695
2.2	1.076079194	2.2	1.075826898	0.023445887
2.3	1.100872249	2.3	1.100530446	0.031048415
2.4	1.12279184	2.4	1.122363303	0.03816709

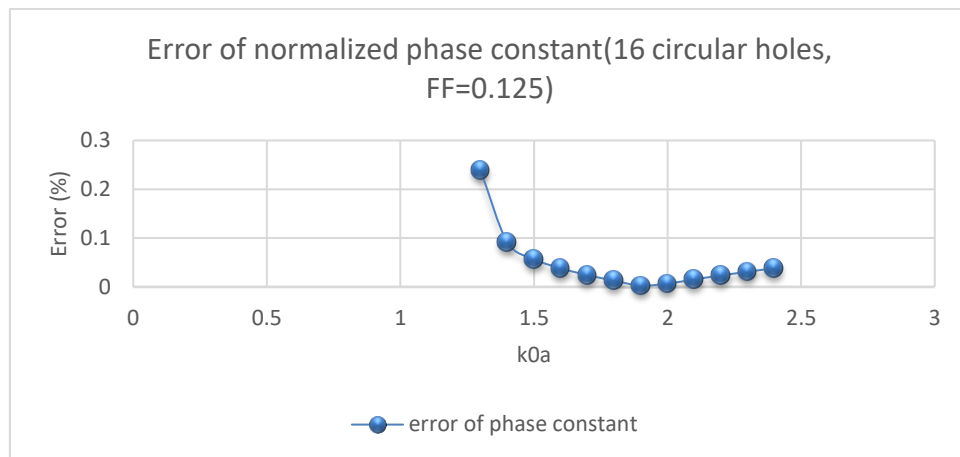


Figure 47 Plot of error of  $\beta/k_0$  versus  $k_0a$  for 16 circular holes with  $FF=0.125$

Table 10 Comparison of some discrete values of first guiding mode between Half dielectric-loaded rectangular waveguide with  $\epsilon_r = 2.069255$  and fully porous dielectric-loaded rectangular waveguide with  $\epsilon_r = 2.25$  and  $FF = 0.125$  for 9 square holes

Half dielectric-Loaded RWG		Half porous dielectric-loaded RWG		Error (%) of $\beta/k_0$
$\epsilon_r = 2.069255$		$\epsilon_r = 2.25$ , $FF=0.125$ , 9 square holes		
$k_0a$	$\beta/k_0$ mode 1	$k_0a$	$\beta/k_0$ mode 1	
1.3	0.351007703	1.3	0.353167678	0.615363975
1.4	0.576474303	1.4	0.577989875	0.262903731
1.5	0.709206817	1.5	0.710493445	0.181417826
1.6	0.802843396	1.6	0.80395496	0.138453473
1.7	0.873942679	1.7	0.874888392	0.1082122
1.8	0.930328049	1.8	0.931107312	0.083762153
1.9	0.976410898	1.9	0.977021473	0.062532518
2	1.014939314	2	1.015379853	0.043405523
2.1	1.047739042	2.1	1.048009959	0.025857271
2.2	1.076079194	2.2	1.076182909	0.009638214
2.3	1.100872249	2.3	1.100813176	0.005366016
2.4	1.12279184	2.4	1.122576235	0.019202566

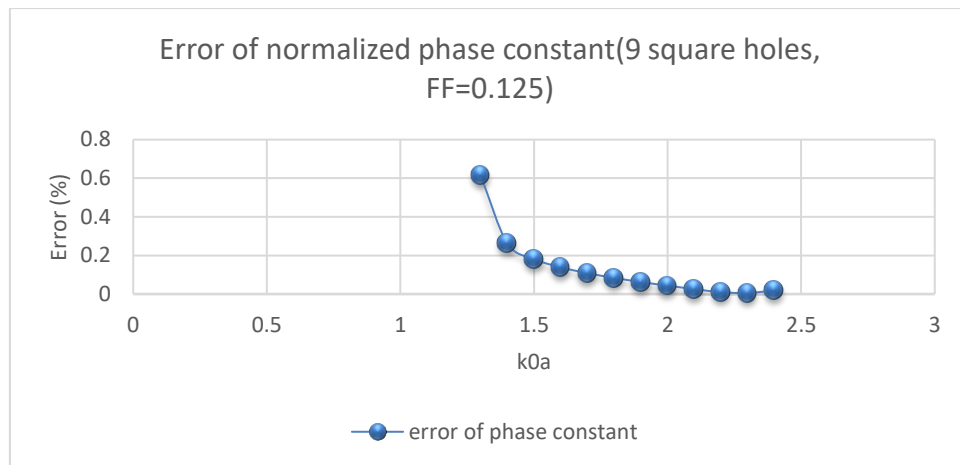


Figure 48 Plot of error of  $\beta/k_0$  versus  $k_0a$  for 9 square holes with FF=0.125

From the comparison results of these three cases, we can conclude that the linear relation between filling factor and relative permittivity of the composite material that form by dielectric material and circular air-tubes are practical in the designs. This relationship is used in the designs of both fully and partially longitudinal porous dielectric-loaded rectangular waveguide and many other application that changing value of relative permittivity of material are required.

**Case 4: Relative permittivity 1.662908 and relative permittivity 2.25 with FF=0.4**

Table 11 Comparison of some discrete values of first guiding mode between

Half dielectric-loaded rectangular waveguide with  $\epsilon_r = 1.662908$  and fully porous dielectric-loaded rectangular waveguide with  $\epsilon_r = 2.25$  and  $FF = 0.4$  for 9 circular holes

Half dielectric-Loaded RWG		Half porous dielectric-loaded RWG		Error (%) of $\beta/k_0$
$\epsilon_r = 1.662908$		$\epsilon_r = 2.25, FF=0.4, 9$ circular holes		
$k_0a$	$\beta/k_0$ mode 1	$k_0a$	$\beta/k_0$ mode 1	
1.4	0.30724291	1.4	0.341063099	11.00763864
1.5	0.510065199	1.5	0.531649325	4.231640563
1.6	0.62977614	1.6	0.647792357	2.860733512
1.7	0.714481936	1.7	0.730766479	2.279209845
1.8	0.778895891	1.8	0.794183197	1.962689142
1.9	0.829971958	1.9	0.844639475	1.767230532
2	0.871646773	2	0.885918227	1.637297861
2.1	0.906387488	2.1	0.920408658	1.546928892
2.2	0.935845386	2.2	0.949718022	1.482364085
2.3	0.961177938	2.3	0.974976903	1.435630551

2.4	0.983224851	2.4	0.997007575	1.401787607
2.5	1.002611755	2.5	1.016423815	1.377607958
2.6	1.019814841	2.6	1.033693415	1.360891536

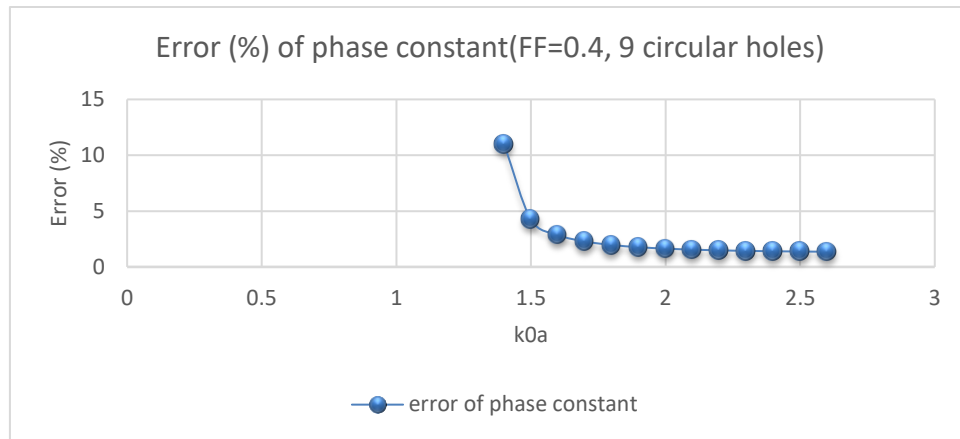


Figure 49 Plot of error of  $\beta/k_0$  versus  $k_0a$  for 9 circular holes with  $FF=0.4$   
Case 5: Relative permittivity 1.1938012 and relative permittivity 2.25 with  $FF=0.8$

Table 12 Comparison of some discrete values of first guiding mode between Half dielectric-loaded rectangular waveguide with  $\epsilon_r = 1.193812$  and fully porous dielectric-loaded rectangular waveguide with  $\epsilon_r = 2.25$  and  $FF = 0.8$  for 9 square holes

Half dielectric-Loaded RWG		Half porous dielectric-loaded RWG		Error (%) of $\beta/k_0$
$\epsilon_r = 1.1938012$		$\epsilon_r = 2.25$ , $FF=0.8$ , 9 square holes		
$k_0a$	$\beta/k_0$ mode 1	$k_0a$	$\beta/k_0$ mode 1	
1.6	0.368441977	1.6	0.368265675	0.047850836
1.7	0.496331511	1.7	0.496216022	0.023268405
1.8	0.5823188	1.8	0.582224259	0.016235266
1.9	0.646266284	1.9	0.646177731	0.013702153
2	0.696281719	2	0.69619104	0.01302333
2.1	0.736657979	2.1	0.736559932	0.013309705
2.2	0.769989581	2.2	0.769880422	0.014176675
2.3	0.797976985	2.3	0.797853863	0.015429201
2.4	0.821797727	2.4	0.821658379	0.016956444
2.5	0.842300499	2.5	0.842143077	0.018689522
2.6	0.860115949	2.6	0.859938918	0.02058226
2.7	0.875724173	2.7	0.875526245	0.022601548
2.8	0.889497939	2.8	0.889278036	0.024722142
2.9	0.901731491	2.9	0.901488712	0.026923687

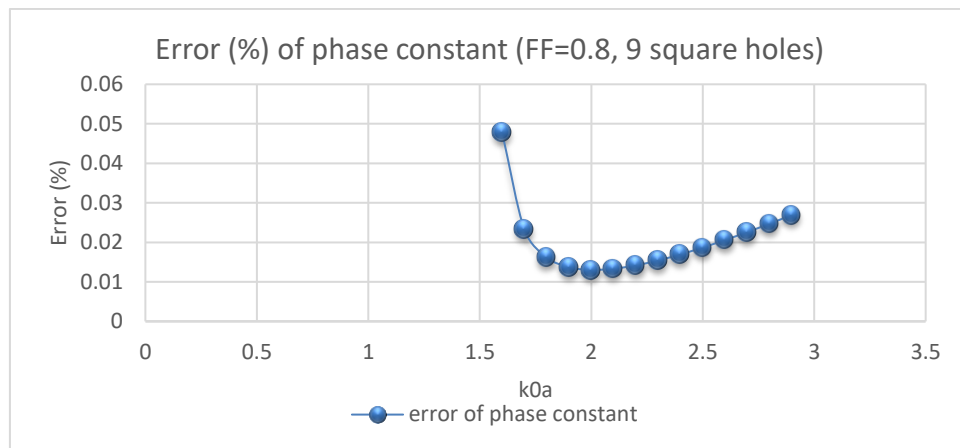


Figure 50 Plot of error of  $\beta/k_0$  versus  $k_0a$  for 9 square holes with FF=0.8

## 6.2. Designs by changing topology of porous dielectric to get target cutoff frequency and bandwidth

The dispersion characteristic of fully porous dielectric-loaded rectangular waveguide is the same as dispersion characteristic of its equivalent fully dielectric-loaded rectangular waveguide. After we know the relation between filling factor and effective relative permittivity of the composite material, we can design fully porous dielectric-loaded rectangular waveguide with targeted cutoff frequency of the first and second guiding mode by computed the require effective permittivity. This permittivity can be calculated from closed-form solution of rectangular waveguide.

By knowing the required value of effective permittivity, we can find its pair value of filling factor to use in the designs. We can change the topology of dielectric material in the waveguide to get specific value of filling factor. Hence, we can get our desired value of cutoff frequency.

From simulation results, the single mode bandwidth of fully porous dielectric-loaded rectangular waveguide always equal to value of the first cutoff frequency. So, the single mode bandwidth of our proposed waveguide can be computed from the chosen value of first cutoff frequency.

Example: we have dielectric material with relative permittivity  $\epsilon_r = 2.25$  to fully load in any rectangular waveguide with cross-section  $2a \times a$ .

If we fully insert this homogenous material into waveguide's cross-section, we can get only one specific value of  $k_0a$ . This value can be calculated from dispersion relation as:

$$(k_0a)_{first\ cutoff} = \frac{\pi}{2\sqrt{\epsilon_r}} = \frac{\pi}{2\sqrt{2.25}} = 1.04719$$

If we fully insert this material and drill some small air-tubes in cross-section of waveguide, we can choose the desirable value of  $k_0a$  at the first cutoff in the range around 1.05 to 1.56 by choosing filling factor from 0 to 1. The relation between  $k_0a$  at first cutoff and relative permittivity of composite material are calculated from

formula:  $\epsilon_r = \left(\frac{\pi}{2k_0a}\right)^2$  with range of  $\epsilon_r$  are chosen from 1 to 2.25.

WR90 has cross-section  $2.286\text{cm} \times 1.143\text{cm}$ . The unit length  $a = 1.143\text{cm}$ . If WR90 fully filled with dielectric material  $\epsilon_r = 2.25$  and we want cutoff frequency  $f_c = 4.9333\text{GHz}$  we can do the following step:

Step 1: Calculate  $(k_0a)_{first\ cutoff}$

$$(k_0a)_{first\ cutoff} = \frac{2\pi f_c a}{c} = \frac{2\pi(4.9333\text{GHz})(1.143\text{cm})}{3 \times 10^8 \text{ m/s}} = 1.181$$

Step 2: Find required value of effective permittivity

$$\epsilon_{eff} = \left(\frac{\pi}{2(k_0a)_{first\ cutoff}}\right)^2 = 1.76879$$

Step 3: Find pair value of effective permittivity and FF

From Figure 29 fit line equation is  $y = -1.2646x + 2.2114$ . If we want  $y = 1.76879$ , we need  $x = 0.35$ . So, the required FF=0.35.

Step 4: Choose number and size of holes in order to get FF=0.35

In this case we choose 18 air-tubes with radius  $r = 0.11126a$ .

After simulation and comparison with result from dispersion relation, we see that the value of error around 0.5%.



## CHAPTER VII CONCLUSION

Numerical experiments of modal analysis of porous dielectric-loaded rectangular waveguides have been investigated by the finite element method. The cutoff frequency of the fundamental mode and single mode operation bandwidth in longitudinal porous dielectric-loaded rectangular waveguides depend on porosity or filling factor of air-tubes in dielectric material. By increasing filling factor, the cutoff frequencies can be increased which enable us to miniaturize the waveguide with desirable cutoff frequency.

This is useful when we cannot find the dielectric material with required value of relative permittivity to load in the waveguide. We can use the consisting dielectric material and drill it with specific value of filling factor to get the targeted value of effective relative permittivity of the composite material.

This kind of waveguide with the same filling factor has the same guiding characteristic no matter the shape or numbers of holes are different. But notice that this condition can be applied while the sizes of the holes are small enough compare to the wavelength at the first cutoff.

One specific value of filling factor is equivalent to one specific value relative permittivity. We can change the dispersion characteristic of porous dielectric-loaded rectangular waveguide by changing the topology of its air-tubes. Table of relationship between filling factor and effective relative permittivity of composite material is important in practical. In order to optimize the cutoff frequency and bandwidth of porous dielectric-loaded waveguide, we need to see what value of filling factor is require to get desirable of relative permittivity. This value of chosen permittivity will give use the desirable dispersion characteristic.

In the future, we want to construct and measure the prototype of the proposed porous dielectric-loaded waveguide structure to verified the results with our results

from simulation. Anyway, we want to use the mathematic tool to analyze the relationship between the effective relative permittivity and filling factor of inhomogeneous medium.



## REFERENCES

1. Yu, Z. *The miniaturization of rectangular waveguide*. in *Microwave and Millimeter Wave Technology (ICMMT), 2010 International Conference on*. 2010.
2. Cheng-Cheh, Y. and C. Tah-Hsiung, *Analysis of dielectric-loaded waveguide*. IEEE Transactions on Microwave Theory and Techniques, 1990. **38**(9): p. 1333-1338.
3. Chatterjee, S.K. and R. Chatterjee, *Dielectric loaded waveguides - a review of theoretical solutions*. Radio and Electronic Engineer, 1965. **30**(3): p. 145-160.
4. Bai, J., et al. *Terahertz Porous Fibers with Random Core Distributions*. in *2010 Symposium on Photonics and Optoelectronics*. 2010.
5. Passaro, D., et al., *All-Silica Hollow-Core Microstructured Bragg Fibers for Biosensor Application*. IEEE Sensors Journal, 2008. **8**(7): p. 1280-1286.
6. Fan, J., et al., *Predicting Mode Properties of Porous-Core Honeycomb Bandgap THz Fibers by Semi-Analytical Theory*. Journal of Lightwave Technology, 2015. **33**(10): p. 1931-1936.
7. Fujii, G., T. Ueta, and M. Mizuno. *Finite element analysis for laser action in random porous media*. in *Advanced Electromagnetic Materials in Microwaves and Optics (METAMATERIALS), 2013 7th International Congress on*. 2013.
8. Boucher, Y.G., J. Charrier, and P. Pirasteh, *Modal Analysis of Graded-Index Porous Silicon Slab Waveguides*. IEEE Journal of Quantum Electronics, 2008. **44**(9): p. 886-893.
9. Uthman, M., et al., *Design and Characterization of Low-Loss Porous-Core Photonic Crystal Fiber*. IEEE Photonics Journal, 2012. **4**(6): p. 2315-2325.
10. Kharkovsky, S., et al., *Microwave Dielectric-Loaded Rectangular Waveguide Resonator for Depth Evaluation of Shallow Flaws in Metals*. IEEE Transactions on Instrumentation and Measurement, 2011. **60**(12): p. 3923-3930.
11. Islam, M.A. and S. Kharkovsky. *Determination of dielectric permittivity of concrete using microwave dielectric-loaded dual-waveguide sensor for infrastructure health monitoring*. in *2016 International Conference on Electromagnetics in Advanced Applications (ICEAA)*. 2016.
12. Leong, M.S., P.S. Kooi, and T.S. Yeo, *Tunable double-ended dielectric-loaded microwave resonator for frequency-stabilisation applications*. Microwaves, Optics and Antennas, IEE Proceedings H, 1981. **128**(4): p. 213-217.
13. Hee Yong, H. and Y. Sang-Won, *Novel  $TE_{10\delta}$  rectangular-waveguide-type resonators and their bandpass filter applications*. IEEE Transactions on Microwave Theory and Techniques, 2002. **50**(7): p. 1821-1831.
14. Lier, E. and C. Stoffels, *Propagation and radiation characteristics of rectangular dielectric-loaded hybrid mode horn*. IEE Proceedings H - Microwaves, Antennas and Propagation, 1991. **138**(5): p. 407-411.
15. Angkaew, T., M. Matsuhara, and N. Kumagai, *Finite-Element Analysis of Waveguide Modes: A Novel Approach that Eliminates Spurious Modes*. IEEE Transactions on Microwave Theory and Techniques, 1987. **35**(2): p. 117-123.
16. Kovacs, A., et al. *Portable optical sensor using tunable optical multilayers*. in *SENSORS, 2013 IEEE*. 2013.
17. Hossain, M.A., et al. *Extremely low loss THz guidance using Kagome lattice porous core photonic crystal fiber*. in *Optical Fiber Communications Conference and Exhibition (OFC), 2015*. 2015.

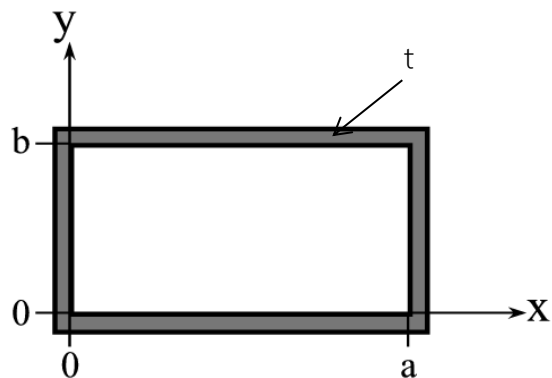
18. Changsoo, H. and L. Milor. *Electric field enhancement caused by porosity in ultra-low-k dielectrics*. in *ISSM 2005, IEEE International Symposium on Semiconductor Manufacturing, 2005*. 2005.
19. Hong, C. and L. Milor. *Porosity-Induced Electric Field Enhancement and Its Impact on Charge Transport in Porous Inter-Metal Dielectrics*. in *2006 IEEE International Reliability Physics Symposium Proceedings*. 2006.
20. Shinji Nishiwaki, T.N., Shinya Kinoshita, Kazuhiro Izui, Masataka Yoshimura, Kazuo Sato, Koichi Hirayama, *Topology optimization for cross-section designs of electromagnetic waveguide targeting guiding characteristics*. *Finite Element in Analysis and Design* 2009. **45**.
21. Nguyen, A.N. and H. Shirai. *A numerical method for the estimation of relative permittivity of dielectric materials*. in *2015 International Conference on Electromagnetics in Advanced Applications (ICEAA)*. 2015.
22. Montoya, R.D.M. and N.G. Gomez. *A simple method to estimate relative permittivity and tangent loss of printed circuit board materials*. in *2013 IEEE Latin-America Conference on Communications*. 2013.



## APPENDIX

Some standard rectangular waveguide

Waveguide Designation	a (width) (in)	b (height) (in)	t (thickness of PEC) (in)	$f_{c10}$ (GHz)	frequency range (GHz)
WR975	9.750	4.875	.125	.605	.75 – 1.12
WR650	6.500	3.250	.080	.908	1.12 – 1.70
WR430	4.300	2.150	.080	1.375	1.70 – 2.60
WR284	2.84	1.34	.080	2.08	2.60 – 3.95
WR187	1.872	.872	.064	3.16	3.95 – 5.85
WR137	1.372	.622	.064	4.29	5.85 – 8.20
WR90	.900	.450	.050	6.56	8.2 – 12.4
WR62	.622	.311	.040	9.49	12.4 - 18



## VITA

Jeudy Kean was born in Banteay Meanchey, Cambodia in 1991. He received the Bachelor's Degree of Electrical Engineering from Institute of Technology of Cambodia in 2014. He has been granted a scholarship by AUN/Seed-Net (JICA) to pursue the master's Degree at Chulalongkorn University, Thailand since 2014. He conducted his research with Communication Laboratory at Department of Electrical Engineering, Faculty of Engineering. His research interests is on Electromagnetic Theory and Application, Computational method for Electromagnetic and Analysis of Waveguide.

